Environmental Science
Atmospheres

Accepted Manuscript

This article can be cited before page numbers have been issued, to do this please use: K. Guleria, S. Tiwari and R. Subramanian, *Environ. Sci.: Atmos.*, 2026, DOI: 10.1039/D5EA00138B.

ROYAL SOCIETY OF CHEMISTRY

rsc.li/esatmospheres

View Article Online
DOI: 10.1039/D5EA00138B

Anthropogenic activities are increasing atmospheric levels of halogenated oxygenated volatile organic compounds (X-OVOCs). This exhaustive list includes halogenated esters, alcohols, aldehydes, ketones, and diketones. It is essential to consider degradation and environmental impact. This study compiles kinetic and radiative data for 94 such compounds and provides new lifetime-corrected impact metrics. The findings reveal their atmospheric behaviour and climatic effects, likely helping identify low-impact alternatives to potent gases like SF_6 and guiding environmental regulations.

View Article Online
DOI: 10.1039/D5EA00138B

ARTICLE

Halogenated OVOCs: A Review of Rate Coefficients, Dielectric Strength, and Environmental Impact

Kanika Guleria[ab], Suresh Tiwari[a], and Ranga Subramanian*[a]

Department of Chemistry, Indian Institute of Technology Patna, India 801103

*Email: ranga@iitp.ac.in

Abstract: Anthropogenic activities have increased the atmospheric emissions of halogenated compounds. Some of these are potent greenhouse gases, but their current atmospheric concentrations are low. We assessed the potential risks and hazards of novel chemical substances before their introduction into the environment. Evaluation systems consider both the direct impacts of exposure to new compounds and the indirect effects of their deposition in soil and surface water when evaluating atmospheric hazards and risks. Therefore, in this study, we reviewed previously published rate coefficient values for oxidants such as OH radicals and Cl atoms and their lifetime values for 94 oxygenated halogenated compounds, including halogenated esters, hydrofluoroalcohols, halogenated aldehydes, halogenated carboxylic acids, halogenated ketones, and diketones. We reviewed the previously calculated radiative efficiencies (REs) and global warming potentials (GWPs) of halogenated compounds over 20, 100, and 500-year time horizons, which are summarized in this study. We also calculated the instantaneous and lifetime-corrected REs and GWPs of 45 halogenated compounds that have not been previously mentioned in the literature. This study also includes global temperature change potential (GTP) values for over 94 halogenated compounds across 20, 50, and 100-year time horizons. Among these, we report GTPs, including instantaneous and lifetime-corrected values, for 59 halogenated compounds for the first time in this study. We also calculated the ozone-depleting potential (ODP) values for chlorine-containing 14 halogenated compounds. The calculated ODP values for these 14 halogenated compounds were low. In this study, we also considered the photochemical ozone creation potential (POCP) and acidification potential (AP) of halogenated oxygenated volatile organic compounds (XOVOCs). This review also provides a thorough investigation of the possible replacement of SF_6, a gas frequently used in electric insulation because of its high dielectric strength (DS). To identify an alternative, the DS values of all the compounds were determined and are provided in this review.

Keywords: Ab initio Calculation, Reaction Mechanism, Rate coefficient, GWP, GTP, Dielectric strength

1. Introduction

Chlorofluorocarbons (CFCs) were a group of substances used for various industrial and household purposes in the 1970s. Their impact was confirmed ten years later with the discovery of the Antarctic ozone hole, a less severe but widespread depletion of stratospheric ozone.[1] In general, CFCs have good chemical stability, low toxicity, low flammability, low gas phase thermal conductivity, and decent cost, and hence were used as cleaning solvents, foam-blowing agents, aerosol propellants, refrigerants,

[a] Department of Chemistry, Indian Institute of Technology Patna, India 801103. Corresponding author: ranga@iitp.ac.in
[b] Presently at Department of Chemistry, University Institute of Sciences, Chandigarh University, Mohali-140413, Punjab, India. Email id: kanika.e19098@cumail.in

View Article Online
DOI: 10.1039/D5EA00138B

and fire-extinguishing agents.[2, 3] A ban on ozone-depleting substances was imposed by the Montreal Protocol (1987)[4, 5] and the Kyoto Protocol (1997)[6] to recover stratospheric ozone.

Hydrofluorocarbons (HFCs) and hydrochlorofluorocarbons (HCFCs) were considered replacements for CFCs. HFCs have no ozone depletion potential (ODP), and HCFCs impact stratospheric ozone because they contain chlorine atoms. They are often highly potent greenhouse gases with significant global warming potentials (GWPs) and are frequently characterized by longer atmospheric lifetimes and strong infrared (IR) absorption.[7] Researchers have been motivated to seek innovative alternatives that meet numerous industrial and commercial purposes while having minimal impact on ozone depletion and climate change. Hydrofluorocarbons (HFCs) and perfluorocarbons (PFCs) are considered second-generation alternatives because they do not contain chlorine or bromine atoms that destroy ozone. They have minimal or no tendency to deplete the ozone layer in the atmosphere.[8, 9] HFCs and PFCs have highly significant global warming potentials (GWPs) and are considered potent greenhouse gases (GHGs) in the Kyoto Protocol.[10]

Hydrofluoroethers are used as substitutes for chlorofluorocarbons in various industrial applications, and undergo atmospheric oxidation to form halogenated esters.[11, 12] Atmospheric breakdown of halogenated esters results in the formation of Trifluoroacetic acid (TFA) and its derivatives, HF, and CO_2.[13] TFA is found in surface waters (lakes, rivers, and seas) and in snow, fog, and rainwater samples.[14-16] TFA is considered an omnipresent accumulating component of the hydrosphere and is not a natural element in freshwater environments.[17] TFA may impact aquatic and agricultural systems.[16]

Halogenated oxygenated volatile organic compounds (XOVOCs) are a superior choice owing to the increased reactivity brought about by the presence of an O atom. To evaluate their environmental effects, a better understanding of the atmospheric chemistry of the different XOVOCs is required. The widespread use of these chemicals is anticipated to significantly affect air quality and climate. Many classes of XOVOCs have emerged, including hydrofluoroethers, fluorinated esters, hydrofluoroalcohols, fluorinated aldehydes, fluorinated ketones, fluorinated diketones, and perfluorinated carboxylic acids. These chemicals are considered prospective substitutes for CFCs, HCFCs, and HFCs.[18]

Hydrofluoroalcohols are utilized in various industrial applications, including coatings, paints, adhesives, polymers, waxes, polishes, and the cleaning of electronic components.[19] It is well known that the main oxidation products of hydrofluoroalcohols are fluorinated aldehydes.[20-23] Fluorinated ketones are used in various industries as organic synthesis reagents and fire-extinguishing agents.[24] There are several applications for fluorinated diketones in metallurgy, where they may be utilized as chelating agents, and in the organic synthesis of medications, unique colors, and coatings.[25-28] A possible source of airborne diketones is the metal-organic chemical vapor deposition method.[29] Perfluorinated carboxylic acids are minor products emitted to the atmosphere from the thermolysis of fluoropolymers.[30]

XOVOCs contain C-F bonds, which make them potent and effective greenhouse gases. They efficiently absorb the infrared radiation emitted by the Earth between the "atmospheric transparency window," that is, between 8 and 12 μm in wavelength. Thus, these molecules may contribute to global warming.[31] In the atmosphere below 1400 cm^{-1}, water absorbs infrared (IR) radiation, whereas above 800 cm^{-1}, water and carbon dioxide absorb IR radiation efficiently. Consequently, the Earth's heat radiation can escape in the region between 800 and 1400 cm^{-1}.[32] Different gases have different radiative

View Article Online
DOI: 10.1039/D5EA00138B

efficiencies owing to variations in the wavelength and intensity of their IR absorption bands.

Radiative efficiency (RE), which quantifies the radiative forcing for a unit change in the atmospheric concentration of a gas, is frequently stated as W m^{-2} ppb^{-1} for halocarbons and similar chemicals.[33] For the assessment of radiative efficiency and GWP, precise knowledge of the atmospheric lifetime and IR absorption spectra is necessary to comprehend the severe dangers posed by a chemical as a potent greenhouse gas. A molecule reacts with different atmospheric oxidants, which determines its lifetime in the atmosphere. The GWP of a molecule is defined as the time-integrated radiative forcing resulting from the instantaneous emission of a kilogram of trace gas relative to that of a kilogram of a reference gas, usually CO_2.[34] Depending on where and how strongly the molecule absorbs infrared light, shorter atmospheric lifetimes often translate to lower GWPs.

XOVOCs in the atmosphere are mostly degraded via a reaction with OH radicals during the entire day.[7, 18, 29, 31, 35-38] Although chlorine atoms can contribute to the removal of XOVOCs, their overall impact is is usually negligible due to their much lower atmospheric abundance compared to OH radicals. However, Cl-initiated reactions may still be relevant in some specific environments such as the marine boundary layer, coastal regions, or certain polluted urban areas where elevated chlorine levels have been observed.[18] Therefore, including Cl-initiated pathways provides a more complete understanding of the possible atmospheric fates of XOVOCs under such region-specific conditions.[39] Photolysis and other chemical degradation mechanisms, such as interactions with NO_3 and O_3, are considered minor atmospheric degradation pathways for XOVOCs. Hydroxyl radicals are anticipated to play a vital role in determining atmospheric lifetimes. [34]

The primary goal of this review is to offer a thorough and consistent study of the input variables, such as rate coefficients and lifetimes, needed to determine the atmospheric implication parameters RE, GWP, GTP, ODP, POCP, and AP values for a large number of XOVOCs. This review addressed the kinetic and mechanistic information currently known for the oxidation of oxygenated organic molecules under tropospheric conditions. The atmospheric lifetime and other crucial input parameters required for calculating GWPs, GTPs, and other metrics are also discussed. Atmospheric lifetime values were obtained from the literature. This review presents a detailed analysis of the instantaneous and lifetime-corrected REs of 105 compounds, including the global warming potential, global temperature change potential, photochemical ozone creation potential, and acidification potential of 94 chemical compounds and the ozone depletion potential of 14 chlorinated compounds. This review also examines the dielectric strengths of all halogenated OVOCs to determine their suitability as substitutes for SF_6 in electrical insulation. The dielectric strength (DS) of each compound was determined.

2. Methodology

There are two approaches to determining the rate coefficients and atmospheric implications of XOVOCs: (1) experimental and (2) theoretical. There are two methods for calculating the rate coefficient of organic compounds with OH radicals or Cl atoms experimentally: the absolute and relative rate methods. Here, we briefly discuss each approach.

2.1 Experimental technique

2.1.1 Kinetics study

2.1.1.a Absolute Technique: When the rate constant for OH radicals is determined using an absolute procedure, the OH radicals are produced utilizing either flash photolysis (FP), laser photolysis (LP), or discharge flow (DF) techniques.[40] Since it is necessary to monitor OH radicals as a function of reaction time, the sensitive

View Article Online
DOI: 10.1039/D5EA00138B

pulsed dye laser-induced fluorescence (LIF) method has been used to detect the absolute rate constants of OH reactions in tropospheric environmental contexts.[41] In the FP approach, a xenon (Xe) flash lamp is used to photolyze water vapor directly. The photolyzing light was directed down the axial line to the reaction cell through a quartz window. Argon (Ar) was used as the carrier gas for the FP technique. Similarly, three approaches to OH generation have been studied using LP methods. The first was the production of OH radicals through the reaction $O(^1D) + H_2O \rightarrow 2OH(\cdot)$ (LP-H_2O method), in which $O(^1D)$ atoms were created by photodissociating N_2O using an ArF excimer laser. The second method for producing OH radicals without the use of water was the $O(^1D) + CH_4 \rightarrow OH(\cdot) + CH_3$ reaction (LP-CH_4 method). Third, the LP-H_2O_2 method, which utilizes a KrF excimer laser to photolyze H_2O_2 directly, was investigated. Helium (He) was used as the carrier gas for the LIF method. The experimental setup description and protocol for the kinetic measurements might be found elsewhere.[42-48]

2.1.1.b Relative Rate Technique: Most often, relative rate approaches in smog chamber experiments have been used to evaluate the rate coefficient of OH reactions under tropospheric conditions or in the presence of 1 atm of air.[41] Various techniques have been used to determine the relative rate constants for the reactions of OH radicals with organic molecules.[49-53] The basic concept behind the relative rate approach is that the rate constant for the reaction of a reference chemical with OH radicals must be determined. Subsequently, the competitive response mechanism can be used to analyze the simultaneous decay of the compound of interest and reference compounds in the presence of OH radicals to obtain the rate constant for the compound of interest. Furthermore, the reference rate coefficient is crucial for selecting reference compounds to increase the sensitivity. Taking Z (reference compounds) and A (interest compounds) as examples, the reaction of OH radicals can be described as follows:

$$Z + OH \longrightarrow \text{Products } (k_Z) \quad (1)$$

$$A + OH \longrightarrow \text{Products } (k_A) \quad (2)$$

$$\frac{d[Z]}{dt} = k_Z[OH][Z] \quad (3)$$

$$\frac{d[A]}{dt} = k_A[OH][A] \quad (4)$$

$$\log\frac{[Z_0]}{[Z_t]} = \frac{k_Z}{2.303} \times \int [OH]\,dt \quad (5)$$

$$\log\frac{[A_0]}{[A_t]} = \frac{k_A}{2.303} \times \int [OH]\,dt \quad (6)$$

$$\log\frac{[A_0]}{[A_t]} = \frac{k_Z}{k_A} \times \log\frac{[Z_0]}{[Z_t]} \quad (7)$$

In this case, $[Z_0]$ and $[A_0]$ represent the concentrations of the reference and interest compounds before the light was turned on. $[Z_t]$ and $[A_t]$ represent the corresponding concentrations after light exposure for time t. The reference compounds and interest compounds, along with their second-order rate coefficients for reaction with OH radicals, are denoted by k_Z and k_A.

2.1.2 Atmospheric implication calculation

2.1.2.a Absorption cross-section (σ_i)

Two methods are generally used to compute the absorption cross-sections: experimental techniques and theoretical calculations. In the case of experimental techniques, infrared absorption spectra are usually obtained using analytical infrared instruments in the 4000-400 cm^{-1} mid-infrared region. In general, measurements are obtained using different spectrophotometers, such as a Bomem DA8, a Mattson Sirius, and a Bruker spectrometer, with a stainless-steel cell fitted with KBr windows at room temperature.[54-57] Operating at a spectral resolution of 0.01 to 0.001 cm^{-1}, the spectrometer produced interferograms based on 100 to 1000 co-

View Article Online
DOI: 10.1039/D5EA00138B

added scans.[54] Spectra of the pure vapour or the mixture containing 60–506 hPa (1 hPa = 9.87 × 10^{-4} atm) of N_2 diluent were recorded. The absorption spectrum was measured in two stages: a long path length cell was evacuated to less than 10^{-3} torr to obtain the background spectrum, followed by the sample gas-filled to a specific pressure (5-165 torr).

$$\tau = \ln\left(\frac{I_0}{I}\right) \qquad (8)$$

In the evacuated cell, I represents the background intensity, and I_0 is the intensity of the sample.

$$\tau = \sigma_i \, n \, L \qquad (9)$$

where σ_i is the absorption cross-section ($cm^2/molecule^{-1}$), L is the path length (cm), and n is the number density of the absorbing molecule ($molecule/cm^{-3}$).

$$n = \frac{273.13 \times PL_0}{1013.0 \times T} \qquad (10)$$

In Equation 10, L_0 is the Loschmidt number, which is 2.69 × 10^{19} molecules per cm^3, T is the gas temperature (kelvin), and P is the pressure of the absorber in hectopascal (hPa). Additionally, a comprehensive assessment of atmospheric metrics, including lifetime, Radiative Efficiency (RE), Global Warming Potential (GWP), Global Temperature Change Potential (GTP), Ozone Depletion Potential (ODP), Photo Ozone Creation Potential (POCP), and Dielectric Strength (DS), is provided in the supplementary information.

2.2 Theoretical techniques

2.2.1 Kinetics Calculation:

According to previous investigations,[58-63] the rate coefficients of organic compounds with oxidizing radicals, such as OH radicals, Cl atoms, and NO_3 radicals, were theoretically determined using Gaussian software based on DFT. Gaussian 16 is a software program for calculating electronic energy.[64] GaussView software is used for visualizing structures.[65] First, using DFT methodologies, M06-2X[66-68], BH&HLYP[69], etc., with different basis sets depending on the computational cost as well as accuracy, such as (cc-pVTZ, and aug-cc-pVTZ, etc)[70-73], geometries of stationary points involved in the oxidation of interest (A) organic compounds with oxidants are optimized. The M06-2X approach is reliable for calculating the thermochemistry, reaction mechanisms, and rate coefficient estimations for main-group element atmospheric reactions.[74, 75] Following stationary point optimization and frequency computation using a reaction channel, transition state concepts (one negative frequency) and stable minima on the potential energy surface were confirmed using the vibrational frequencies. Each local minimum was described using real frequencies, and the presence of one imaginary frequency verified the existence of the transition stages. To confirm that the reactants were transformed into their intended products via transition state crossings, intrinsic reaction coordinate (IRC)[76, 77] calculations for all the transition states were performed at the same level of theory. Using the optimized geometries, single-point energy calculations were performed using the high-level coupled-cluster single-double and perturbative triples (CCSD(T))[78] technique with a basis set (depending on accuracy and computational cost) to refine the potential energy surface and obtain more accurate energies.

Rate coefficients are calculated using the canonical variational transition state theory (CVT) for the tropospheric temperature range, considering the atmospheric significance.[79-81] Two methods are used for tunneling corrections: zero-curvature tunneling (ZCT)[81-83] and small curvature tunneling (SCT).[84, 85] Canonical variational theory rate coefficients k^{CVT} (T) are derived by minimizing along the dividing surface (s) at a given temperature (T). They are represented as follows:

$$k^{CVT}(T) = k^{GT}(T,s) \qquad (11)$$

$$k^{GT}(T,s) = \frac{\sigma k_B T Q^{GT}(T,s)}{h \quad \phi^R(T)} \exp\left(-\frac{V_{MEP}^{CVT}(s)}{k_B T}\right) \quad (12)$$

Here, $k^{GT}(T,s)$ is the generalized transition state theory rate coefficient at the dividing surface s, σ is the symmetry factor, k_B is the Boltzmann constant, h is Planck's constant, and $Q^{GT}(T,s)$ is the partition function of the generalized transition state at s with a local zero of energy at $V_{MEP}^{CVT}(s)$. $\phi^R(T)$ is the partition function of the reactants per unit volume. The CVTST rate coefficient is multiplied by the transmission coefficient, κ_T, to account for the tunneling effects. κ_T is calculated with zero-curvature tunneling (ZCT) and small-curvature tunneling (SCT). The modified Arrhenius equation was fitted to the computed CVT/SCT rate coefficients in the temperature range.

$$k = AT^n \exp\left(\frac{-E_a}{RT}\right) \quad (13)$$

where T is the temperature, n is the temperature exponent, R is the universal gas constant, and E_a is the barrier height. A is the Arrhenius prefactor.

2.2.2 Molecular Descriptors Calculations

All compounds included in this review performed geometric optimization and frequency calculations at the B3LYP/6-31G(d,p) theoretical level.[70, 86-99] The Becke 3-parameter, Lee-Yang-Parr (B3LYP) method, a widely used DFT technique, was used to calculate the RE values. The B3LYP functional includes the exchange functional of HF, the empirical correlation functional of Lee, Yang, and Parr, and Becke's empirical exchange functional.[100] Examination of the vibrational frequencies revealed that all frequencies were positive absolute values, indicating that the optimized geometry was a minimum on the potential energy surface at the B3LYP/6-31G(d,p) level of theory. The B3LYP DFT calculations provided a noticeably greater agreement with experimental data. Bravo et al. compared experiment and theory-based DFT calculations throughout the range of 700-1400 cm^{-1}; the parameters of the best-fit line show variations of less than 2% but over 5% for ab initio calculations.[89] Utilizing the frequency and optimized computation of XOVOCs at the B3LYP method and Pople 6-311+G(d,p) basis set, studies of the molecular descriptors such as frontier molecular orbital (FMO), reactivity parameters such as molecular electrostatic potential (MEP), and non-covalent interaction (NCI) were conducted. The FMO, MEP, and NCI analyses were performed using the Multiwfn software.[101] The wavefunction files of the oxygenated organic compounds were obtained using Gaussian 16. Subsequently, these wavefunction files were used as input files for Multiwfn. All isosurface maps were produced using the Visual Molecular Dynamics (VMD) 1.9.3 program based on the results of the Multiwfn analyzer.[102] The B3LYP/6-311+G(d,p) level of theory was used to determine the dielectric strengths (DS) of all oxygenated organic compounds included in this review. According to earlier research, the B3LYP/6-311+G(d,p) level of theory is the most effective DFT method for estimating the dielectric strength (DS). [103-106]

View Article Online DOI: 10.1039/D5EA00138B

3. Results and discussion

3.1 Halogenated Esters

3.1.1 Rate coefficient of Halogenated Esters

The literature rate coefficients and lifetime data for the reactions between halogenated esters and oxidants (OH radicals and Cl atoms) are presented in Tables S2 and S3, respectively. In these supplemental (given in Tables S2 & S3), we reviewed the lifetime values and rate coefficients of various halogenated esters, such as fluoroalkyl formates,[12, 107-112] fluoroalkyl acetates,[113, 114] fluoroalkyl fluoroacetates [115-117] etc. The reactivity of alkyl esters was not significantly affected by the extension of the alkyl chain length, whereas formates, acetates, propionates, and butyrates exhibited a greater chain length dependency.[118-120] Blanco et al. [115] previously showed that the reaction rates of the halogenated esters are greater than those

View Article Online
DOI: 10.1039/D5EA00138B

of the equivalent halocarbons. The ester linkage, -C(O)O-, often activates neighboring C-H bonds. Mechanistic insights show that halogen-atom abstraction plays a modest role in OH-initiated reactions, which mostly occur through hydrogen abstraction, frequently preceded by the formation of hydrogen-bonded complexes.[121, 122] Furthermore, the combined effects of H-atom abstraction and radical addition across the C=C bond exhibit significantly greater rate coefficients in unsaturated halogenated esters, such as fluorinated acrylates and methacrylates, than in their saturated equivalents. In electrophilic addition processes, the -OC(O)R group associated with the double bond activates this bond. Therefore, the π system's electrical density increases owing to the oxygen atom's lone pair of electrons (Figure S4). These results demonstrate how the oxidative existence of halogenated esters in the environment is controlled by electronic structure and substitution patterns.

3.1.2 Atmospheric Fate of Halogenated Esters:

Several halogenated esters have mechanistic data available for hydrogen abstraction, including fluoroalkyl formates,[12, 107-112]fluoroalkyl acetates,[113, 114]and fluoroalkyl fluoroacetates.[115-117]have investigated the use of oxidants such as OH radicals and Cl atoms. The OH radical-initiated atmospheric degradation of the investigated saturated halogenated esters is predicted to result in the generation of halogenated acids, alcohols, aldehydes, and dicarbonyl compounds, which are prone to additional OH reactions and photolysis. Lower molecular weight acids, which are degradation products of halogenated esters, are highly soluble substances that can be rapidly absorbed into cloud droplets, leading to precipitation. [123]

The degradation of halogenated esters with oxidants has been investigated previously, and we have reviewed some of the detailed degradation mechanisms of halogenated esters that fall under the category of saturated halogenated esters. The radical product is generated via -H atom abstraction, and in the case of fluoroalkyl acetates such as $CF_3C(O)$, the OCH_2CH_3 moiety undergoes an α-ester rearrangement via a five-membered ring intermediate to yield the equivalent fluoroacetic acid. And their detailed mechanism is shown in Schematic diagram 3.1.2.a. These radicals may also react directly with O_2 to form the equivalent

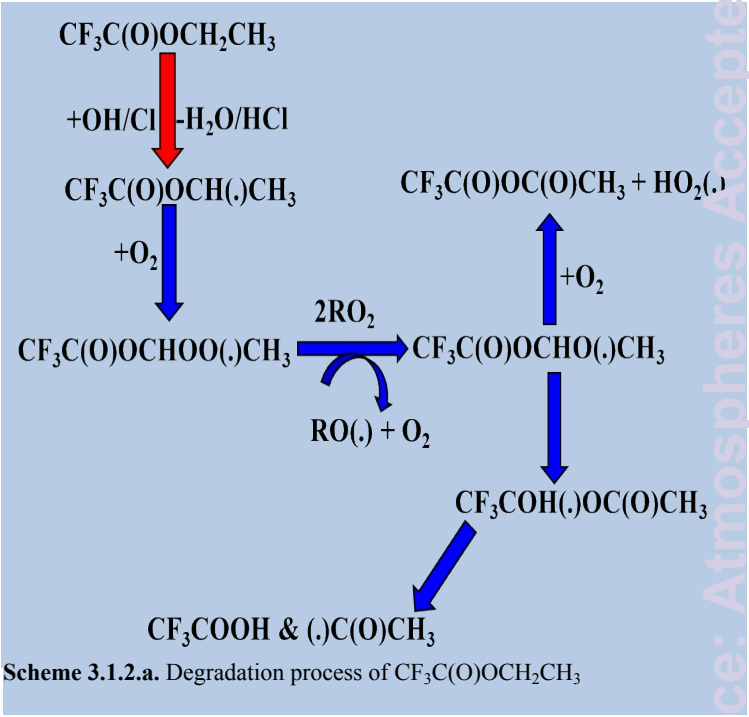

Scheme 3.1.2.a. Degradation process of $CF_3C(O)OCH_2CH_3$

View Article Online
DOI: 10.1039/D5EA00138B

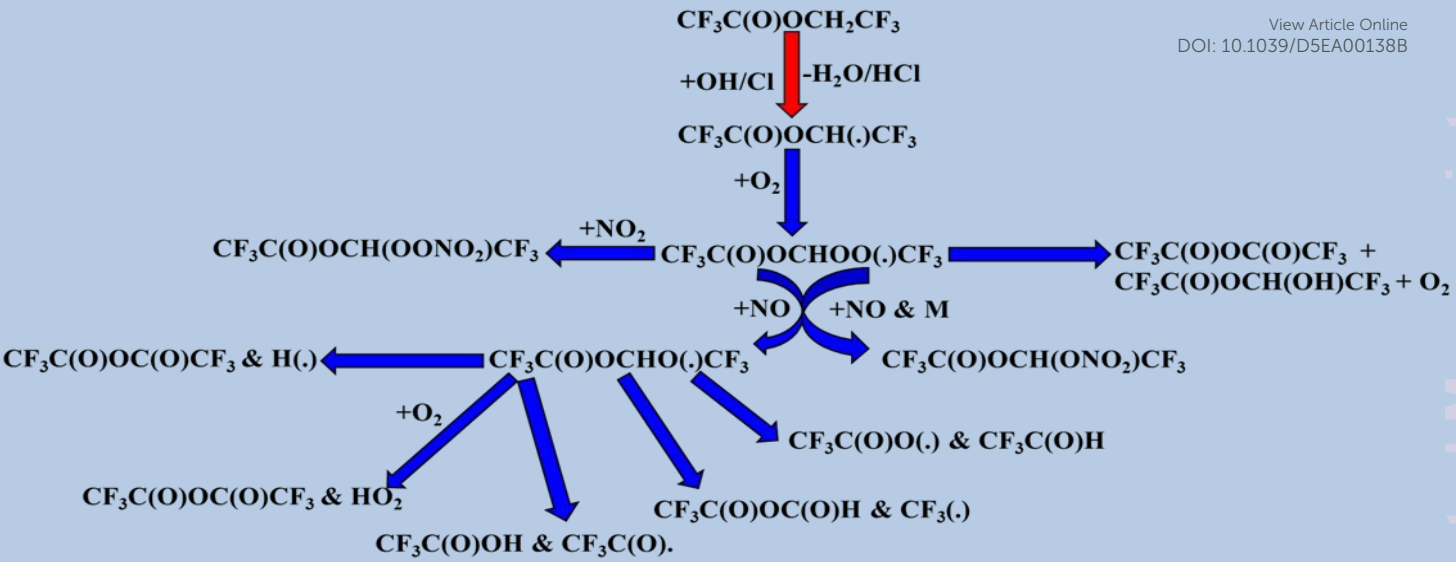

Scheme 3.1.2. b. Degradation process of $CF_3C(O)OCH_2CF_3$

fluoroanhydride.[123] When $-CH_3$ is substituted with a $-CF_3$ group in $CF_3C(O)OCH_2CH_3$, -H abstracts from the $-CH_2$ position using OH radicals to produce the alkyl radical product $CF_3C(O)OCH(.)CF_3$. After that, the peroxy radical $CF_3C(O)OCH(OO.)CF_3$ is produced by the reaction of alkyl radicals with ambient oxygen (Scheme 3.1.2.b). Then, the peroxy radical quickly combines with NO to form NO_2 and, consequently, $CF_3C(O)OCH(O.)CF_3$ radicals. At 296 K and 1 atm atmospheric pressure, 65% of the $CF_3C(O)OCH(OO.)CF_3$ radicals react with ambient O_2 molecule. Subsequently, they produce $CF_3C(O)OCH(O)CF_3$, and 18% undergo through α-ester rearrangement to produce $CF_3C(O)OH$ and $CF_3C(O)$, radicals. The fates of the remaining 17% is still unknown.[124] Prior research on the atmospheric degradation of methyl dichloroacetate's ($CHCl_2C(O)OCH_3$) has concentrated on its reactivity with OH radicals. The methyl group ($-CH_3$) or the α-position next to the carbonyl ($-CHCl_2$) are the two main routes for hydrogen abstraction. $CCl_2(.)COOCH_3$ is the radical intermediate that is produced when abstraction at the α-site is energetically favored. The mechanistic preference highlights the role of halogen substitution in stabilizing radical intermediates and influencing the oxidative routes of halogenated esters in the environment. Following the formation of alkyl radical products (Scheme 3.1.2.c.), these radicals react with atmospheric oxygen to produce the peroxy radical $CCl_2OO(.)COOCH_3$, which further reacts with NO to produce the molecules NO_2 & $CCl_2(O)C(O)OCH_3$.[125, 126] Furthermore, our research group also investigated the atmospheric deterioration of $CF_xH_{3-x}CF_2C(O)OCH_3$ ($x = 3$ *and* 2) reaction kinetics, and radical product degradation with OH radicals. After forming alkyl radical products, they reacted with ambient oxygen to generate $CF_xH_{3-x}CF_2C(O)OCH_2(OO)$ radicals. Following their synthesis, $CF_xH_{3-x}CF_2C(O)OCH_2(OO)$ radicals react with other radicals through several paths to produce halo alkoxy radicals (see Scheme 3.1.2.d).[87]

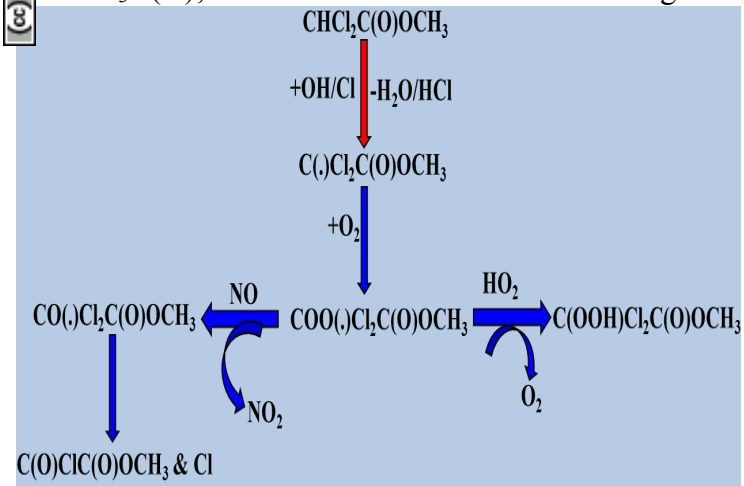

Scheme 3.1.2. c. Degradation process of $CHCl_2(O)C(O)OCH_3$

View Article Online
DOI: 10.1039/D5EA00138B

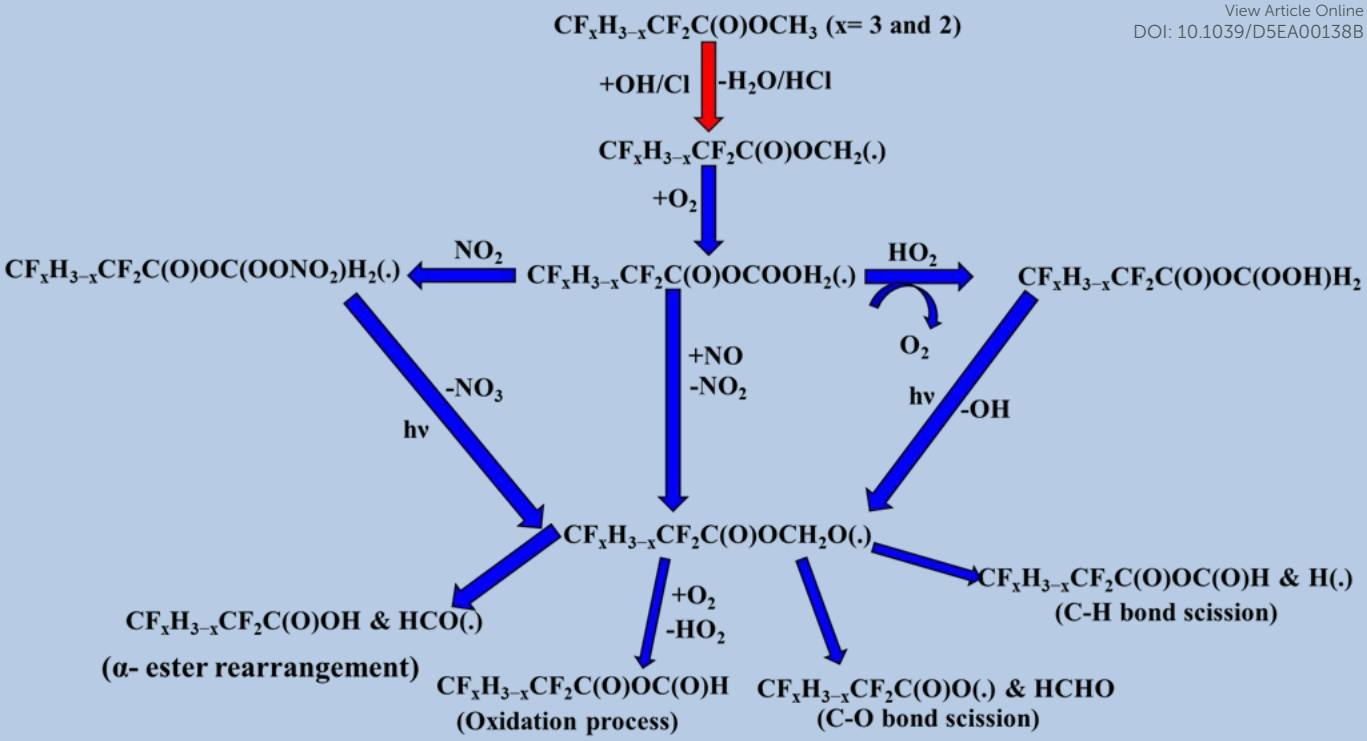

Scheme 3.1.2. d. Degradation process of $CF_xH_{3-x}CF_2C(O)OCH_3$

Unsaturated halogenated esters degrade to halogenated glyoxylate and pyruvate, which may further react with OH or Cl to generate halogenated aldehydes and contribute to the generation of ozone and secondary organic aerosols (SOA). The halogenated carboxylic acids are potential contaminants believed to be produced by the oxidation of halogenated glyoxylates and pyruvates; their detailed degradation mechanism was studied by Rodriguez et al.[127], Teruel et al.[114] and Wallington et al.[128]

3.1.3 Atmospheric implications of halogenated esters

The atmospheric lifetimes of halogenated esters were calculated by determining the rate coefficients for reactions with OH radicals and Cl atoms. Although OH oxidation prevails in most situations, Cl atom reactions play an important role in coastal and marine boundary layer conditions. The total lifetime duration for compounds with reported Cl rate constants was calculated by combining the OH- and Cl-initiated pathways, whereas lifetimes without such data were based only on OH reactivity. The calculated lifetimes of the 41 halogenated esters are presented in Table S2. The lifetime of considered halogenated esters varies from 5 hours for $CH_2=C(CH_3)C(O)OCH_2CF_3$ reported by Tovar and Teruel[114] to 3.6 years for $HC(O)OCF_3$, $HC(O)OCF_2CF_3$.[34] Unsaturated esters like $CF_3C(O)OCH=CH_2$, $CF_3C(O)OCH_2CH=CH_2$, $CH_2=C(CH_3)C(O)OCH(CF_3)_2$, $CH_2=C(CH_3)C(O)OCH_2CF_3$, $CH_2=CHC(O)OCH_2CF_3$, $CH_2=CHC(O)OCH(CF_3)_2$, $CH_2=CHC(O)O(CH_2)_2C_4F_9$ have negligible lifetime because of the presence of unsaturation. Compared to their saturated counterparts, unsaturated halogenated esters have much shorter lifetimes because of the extra OH addition channel across the C=C bond, which increases overall their reactivity. In contrast, due to the absence of such addition routes, saturated esters exhibit considerably longer atmospheric persistence. [127] These differences were further demonstrated by photochemical ozone formation potential (POCP) measurements. Compared to ethene (POCP = 100), most

View Article Online
DOI: 10.1039/D5EA00138B

halogenated esters have a low POCP, suggesting a restricted role in tropospheric ozone generation and minimal risk to biological health or air quality. Nevertheless, the POCP values of unsaturated fluorinated acrylates and methacrylates are significantly greater, indicating their dual reactivity through H-abstraction and OH addition processes. These results show that the atmospheric lifetimes and subsequent ozone production potential of halogenated esters are controlled by their structural characteristics, especially unsaturation.

The optimized geometry, infrared absorption cross-section, molecular electrostatic potential (MEP), and frontier molecular orbital (FMO) surfaces for $HCOOCHFCF_2CF_3$ are provided in Figure 1 for representation, while the corresponding data for the other halogenated esters are given in Supplementary Figure S2, S3 and S4. The Absorption cross-sections and resultant radiative efficiencies (REs) for all 52 compounds were determined using calculated spectra obtained from their infrared frequencies and intensities. This enabled the computation of GWPs over 20, 100, and 500-year time-horizon could be computed for 41 esters, While estimates for remaining ones including $FC(O)OCFH_2$, $FC(O)OCF_2H$,$FC(O)OCF_3$,$FC(O)OCF_2CF_3$,$FC(O)OCH_2CF_3$,$FC(O)OCF_2CF_2CF_3$,$CF_3C(O)OCF_3$,$CF_3C(O)OCF_2CF_3$,$CF_3C(O)OCH(CF_3)_2$, and $CF_3C(O)OPh$, are still unavailable due to their expected fast atmospheric elimination by wet deposition processes. These findings highlight the crucial role of kinetic measurements and quantum-chemical predictions in revealing the radiative forcing and climate significance of halogenated esters.[34] The vibrational properties of halogenated esters within the atmospheric infrared window (700-1400 cm^{-1}) greatly influence their GWPs. Since this area has considerable IR absorption, and compounds with C–F, C–Cl, C–Br, S–F, and N–F bonds have enhanced GWPs, with fluorine substitution having the significant impact. While chlorinated equivalents show noticeably less absorption, increasing the amount of fluorine atoms increases the intensity of IR absorption (see Table S4) and, thus, the radiative efficiency (RE). $CHCl_2C(O)OCH_3$, for instance, has a comparatively low intensity (approximately 618 km/mole), which is in line with its lower RE and GWP. We also calculated the instantaneous and lifetime-corrected REs and GWPs of the 17 halogenated esters. However, these aspects have not yet been reported in the literature. The calculated GWP values for unsaturated halogenated esters over 20, 100, and 500-year time horizons were negligible because of their short atmospheric lifetimes. From Tables S3 and S5, it is evident that both RE and GWP exhibits a positive dependence on the atmospheric lifetime. This behavior is strongly influenced by the underlying characteristics of the XOVOCs. In particular, the substitution of hydrogen with fluorine alters the molecular dipole moment, vibrational mode, and chemical reactivity. These changes generally decrease the OH reaction rate coefficient, thereby increasing the atmospheric lifetime, while simultaneously enhancing RE and GWP. In addition

View Article Online
DOI: 10.1039/D5EA00138B

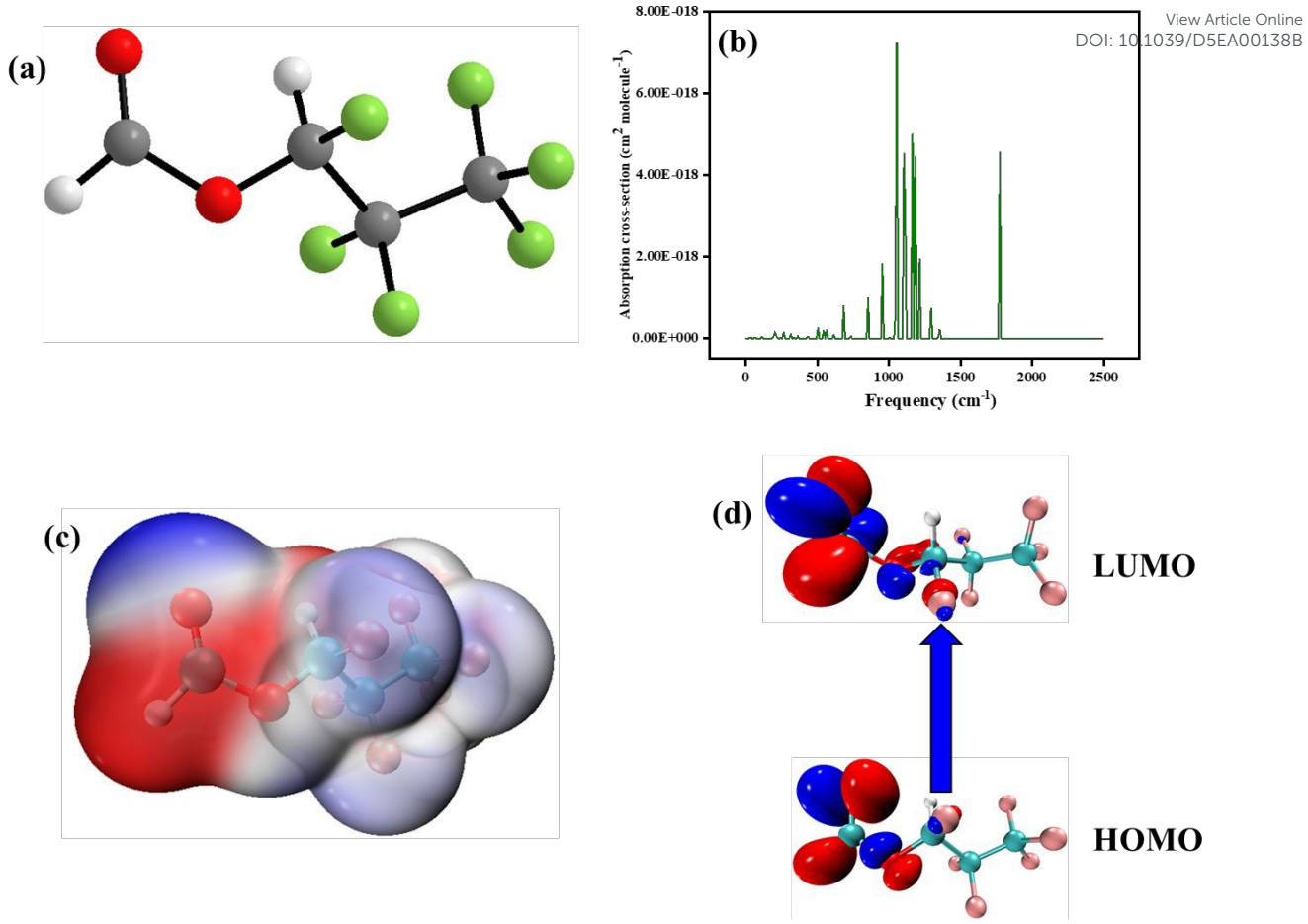

Figure 1. $HC(O)OCHFCF_2CF_3$ molecular descriptor. (a) Optimized Geometry (b). Absorption cross-section (c) Molecular electrostatic potential (d) Frontier Molecular Orbital

to the ODPs of four chlorine-containing esters and the AP of 41 fluorinated esters, the GTPs of 41 halogenated esters were assessed (Table S6) across time horizons of 20, 50, and 100 years. For the first time, 19 halogenated esters were reported, and both instantaneous and lifetime-corrected GTPs were measured. The GTP values scale with the atmospheric lifetime (τ) in accordance with GWP trends, whereas unsaturated fluorinated acrylates and methacrylates exhibit insignificant GTPs because of their short lifetimes. Because the acidification potentials of fluorinated esters are identical to or higher than those of SO_2, it is possible that the atmospheric breakdown of these esters may lead to the acidification of rainfall. These results emphasize the broader climatic and environmental consequences of halogenated esters, which extend beyond greenhouse forcing to encompass phenomena such as acidification and ozone depletion.

3.2 Halogenated alcohols

3.2.1 Rate coefficient of halogenated alcohols

Halogenated alcohols are mainly eliminated from the atmosphere via oxidation by OH radicals and Cl atoms in coastal and marine boundary layer areas. H-atom abstraction at sites close to the hydroxyl group is often less advantageous than at other locations, according to rate coefficients and lifetimes derived from the literature (Tables S9 and S10). This is because the radicals produced from the carbon-centered radical were more polarizable, which made them more stable than those produced from the oxygen-centered radical. Reaction rates for $CF_3(CH_2)_nOH$ (n = 0-3) show the effects of both chain extension and electron-withdrawing,

View Article Online
DOI: 10.1039/D5EA00138B

increasing with carbon chain length while decreasing with more fluorine substitution.[129-132] The most electron-deficient locations are hydrogen atoms, which makes them more susceptible to abstraction than F or Cl atoms, according to electrostatic potential maps (see Figure S7). Although the -OCH_2- reactivity marginally decreases with increasing distance from the OH group, the higher reactivity of the β- and γ-CH_2 groups in compared to that of unsubstituted alkanes further emphasizes the activating impact of the hydroxyl functionality. These mechanistic tendencies, which relate the electronic structure to the observed reactivity patterns in halogenated alcohols, are supported by a comparison of the calculated frontier molecular orbital (FMO) energy gaps with experimental rate coefficient data. The FMO diagram is presented in Figure S8, and the FMO energy gap are listed in Table S8.

3.2.2 Atmospheric fate of halogenated alcohols:

The formation of fluorinated aldehydes and perfluorinated carboxylic acids by the tropospheric oxidation of halogenated alcohols with OH radicals and Cl atoms has been reported in previous studies.[20, 31, 129-132] Based on earlier research, the OH-initiated oxidation reaction mechanism of $CF_3C(CH_3)OHCF_3$, $(CF_3)_2CHOH$, and $(CF_3)_3COH$ was examined here.[130, 133-135] The radical product $(CF_3)_2COHC(.)H_2$ is the initial byproduct of the oxidation of $CF_3CXOHCF_3$ (X = CH_3) with atmospheric oxidants. Compared to the -OH position, -H abstraction from the -CH_3 position was preferred. Once alkyl radicals like $(CF_3)_2COHC(.)H_2$ reacts with ambient oxygen in the atmosphere to produce peroxy radicals, such as $(CF_3)_2COHCH_2OO(.)$ moiety. In a NO-rich environment, they react with peroxy radicals to produce alkoxy radicals $(CF_3)_2COHCH_2O(.)$, which then break down the C-O bond to produce formaldehyde and $(CF_3)_2C(.)OH$. The presence of an O_2 molecule causes $(CF_3)_2C(.)OH$ undergoes HO_2 elimination to produce $CF_3C(O)CF_3$ via the following reaction pathways. When $CF_3CXOHCF_3$ (X = H) reacts with oxidizing radicals, the alkyl radical product $(CF_3)_2C(.)OH$ is formed primarily because -H abstraction from the -CH group is easier than that from the -OH position. Alkyl radicals react with ambient O_2 to eliminate HO_2 and generate $CF_3C(O)CF_3$. A minor product can produce fluorinated peroxy radicals $(CF_3)COO(.)OH$; if these are persistent, they can form fluorinated

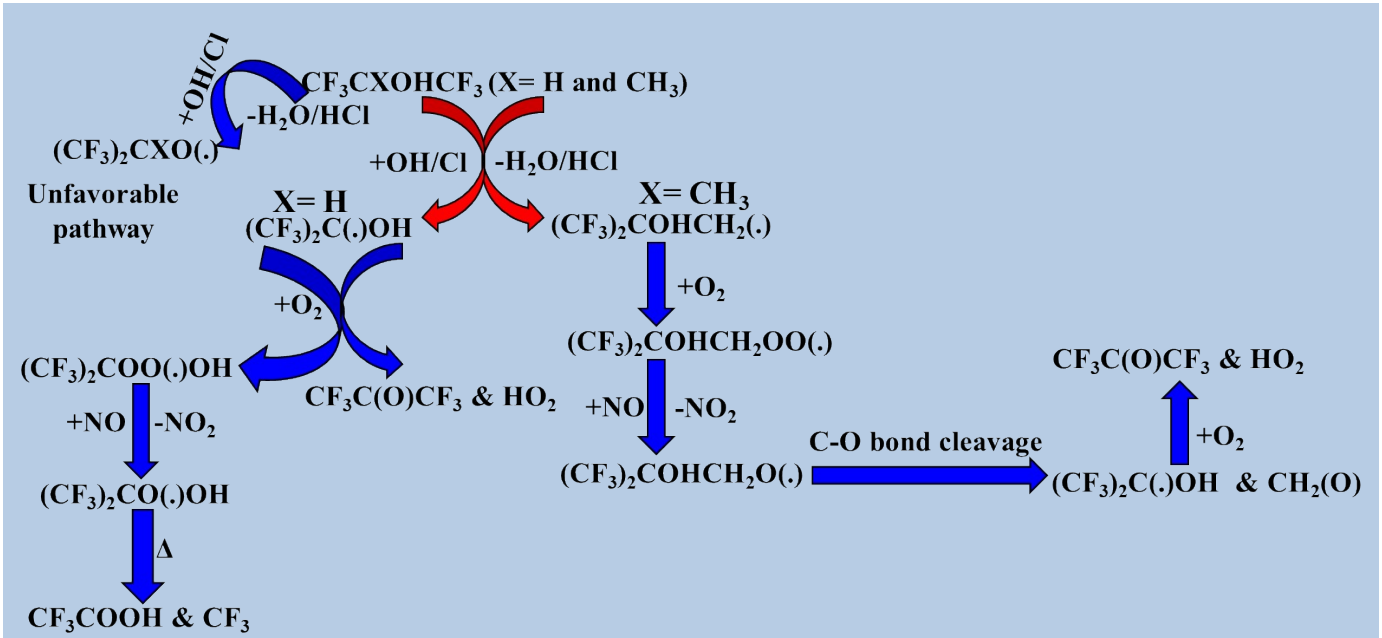

Scheme 3.2.2. a Degradation process of $CF_3CXOHCF_3$ X= H and CH_3

View Article Online
DOI: 10.1039/D5EA00138B

carboxylic acids . Detailed degradation pathways for $CF_3CXOHCF_3$ (X= H and CH_3) are shown in scheme 3.2.2. a. We utilized information gathered from previous research to determine the atmospheric degradation pathways of $CF_3(CX_2)_nCH_2OH$ ($X = H, F, and\ n = 0, 1, and\ 2$) and $CF_3(CF_2)_nCH_2CH_2OH$ ($n = 4, 6, and\ 8$) degradation by oxidizing radicals such as Cl atoms and OH radicals.[131, 136] In this case, two positions allow for -H abstraction: one from -CH_2O and another from -OH. Reaction channels with the -CH_2O position were more frequently observed than those with the -OH position. The first stage is the production of alkyl radicals, which are then broken down in four distinct ways: reaction with oxygen, C-C bond breaking, C-H bond breakage, and C-O bond breakage. Data from earlier research indicate that the degradation processes of CHF_2CH_2OH, CH_2FCH_2OH, and $CHF_2CF_2CH_2OH$ are similar to a sequence of $CF_3(CX_2)_nCH_2OH$ ($where\ X = H, F, and\ n = 0, 1, and\ 2$) that degrades via four distinct pathways.[18, 31]

Mabury et al.[156] previously discussed the degradation of $C_4F_9SO_2N(CH_3)CH_2CH_2OH$ by OH radicals. As shown in the schematic illustration (3.2.2.c.), when alkyl radicals react with ambient oxygen, they remove HO_2, produce fluorinated aldehydes, and a second pathway results in the addition of OH radicals. In this pathway, the major byproducts are perfluorinated acids and alcohols. Perfluorinated acids are environmentally persistent and withstand oxidation, hydrolysis, and reduction in biotic and abiotic environments. Fluorinated aldehydes are the primary oxidation products of fluorinated alcohols. Secondary oxidation products have been reported to be CHFO or CF_2O, which will be absorbed into droplets/aerosols and hydrolyzed within days to provide CO, CO_2, and HF.[136]

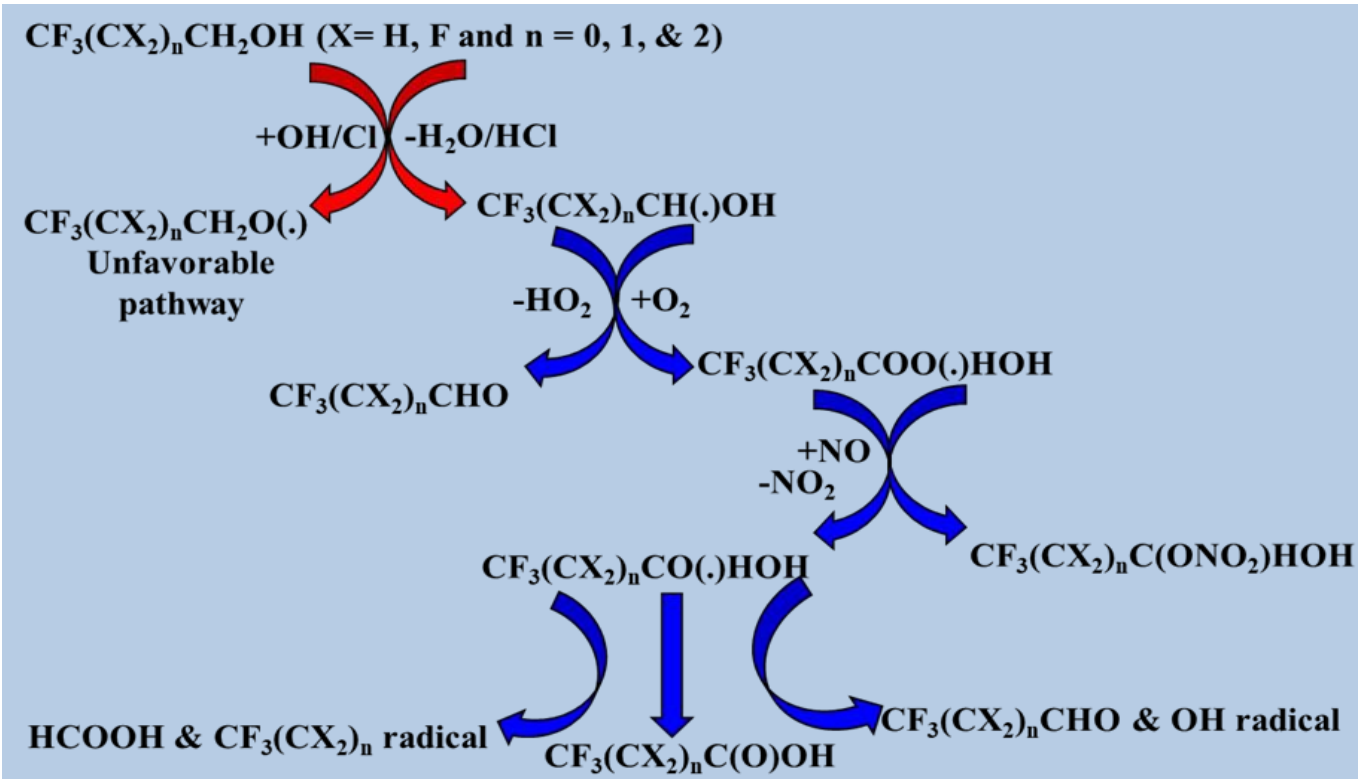

Scheme 3.2.2. b. Degradation process of $CF_3(CX_2)_nCH_2OH$

View Article Online
DOI: 10.1039/D5EA00138B

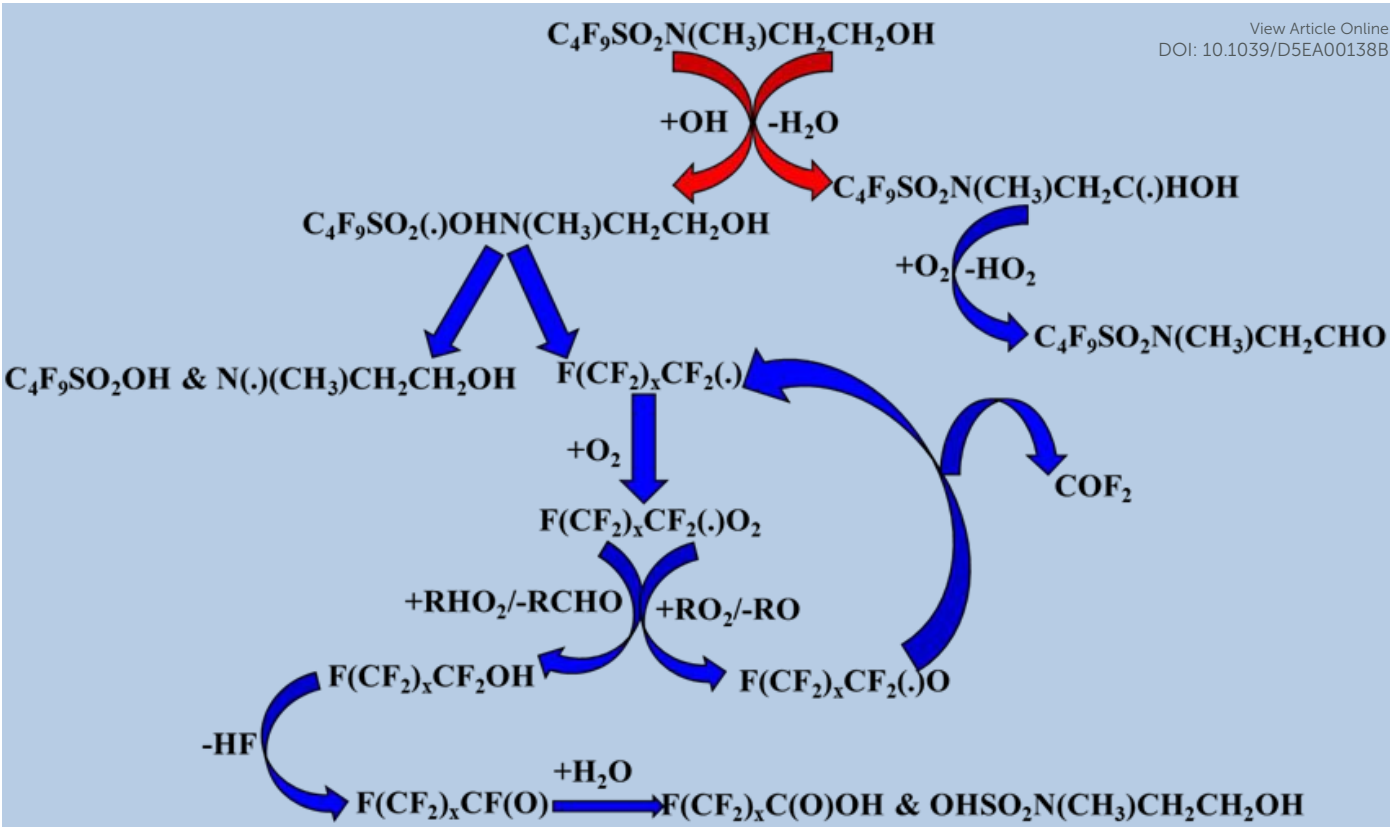

Scheme 3.2.2. c. Degradation process of $C_4F_9SO_2N(CH_3)CH_2CH_2OH$

3.2.3 Atmospheric Implications of halogenated alcohols

Rajakumar *et al.*[135], Garzon *et al.*[129], Pan *et al.*[131], and Chandra *et al.*[137] have shown atmospheric lifetimes for several types of halogenated alcohols produced by both OH radicals and Cl atoms, with Cl-driven values assessed under two conditions: global mean chlorine concentrations and elevated concentrations typical of the marine boundary layer. As shown in Table S10, the total lifetime of each compound was determined by combining the OH- and Cl-mediated pathways. Based on the global average [Cl], the lowest reported total lifetime value is 10 days for $CF_3CH_2CH_2OH$, and the highest lifetime is 46 years for $(CF_3)_3COH$. Considering the chlorine concentration in marine boundary layers, the lowest estimated atmospheric lifetime was 0.0028 years for the $CF_3CH_2CH_2CH_2OH$ molecule reported by Pan *et al.*[131]. The highest value is 2.9 years for the $CF_3C(CH_3)OHCF_3$ molecule reported by Rajakumar *et al.*[135] These findings emphasize the importance of local halogen chemistry in determining persistence. We estimated the POCP values for 19 halogenated alcohols, which are listed in Table S9. Table S9 shows that halogenated alcohols have considerably lower POCP values than ethene (100).

IR absorption spectra and subsequent calculation of the absorption cross sections, REs, and GWPs are presented in (Tables S11–S13, Figures S6 and S9). Fluorine substitution, as predicted, increased the RE values because of greater absorption (see Figure S8) in the atmospheric window (700-1400 cm^{-1}). Using the absorption cross-section calculation, we summarized the instantaneous and lifetime-corrected REs and GWP in Table S12. Rajakumar *et al.*[135], Pan *et al.*[84], and Chandra *et al.*[18] calculated two different GWP values at two different [Cl] atom concentrations, one at the global average concentration (620 molecules per cm^3)[138] and the other in marine boundary layers (1200 molecules per cm^3)[138] for $CF_3C(CH_3)OHCF_3$,

View Article Online
DOI: 10.1039/D5EA00138B

$CF_3CH_2CH_2CH_2OH$, and $CHF_2CF_2CH_2OH$. The GWP values of halogenated alcohols are significantly lower, but $CF_2CF_2CF_2CH_2OH$ and $(CF_3)_3COH$ molecules have comparatively high GWP values, which are comparable to CFC-11, with a GWP value of 6330 at 20 years' time horizons, highlighting their possible climatic significance owing to their high atmospheric lifetime. The GTP values of 19 halogenated alcohols over 20, 50, and 100 years are listed in both instantaneous and lifetime-corrected forms in Table S11, among which we report GTP values of seven halogenated alcohols for the first time. Furthermore, the APs of 19 halogenated alcohols and the ozone depletion potential (ODP) of $CHCl_2CH_2OH$ were assessed. Rainwater acidification may be caused by halogenated alcohol breakdown products, as the AP values continuously outperformed SO_2. These results demonstrate that although the majority of halogenated alcohols have no direct greenhouse or ozone-depleting effects, highly fluorinated congeners are hazardous to the climate and environment.

3.3 Halogenated aldehydes

3.3.1 Rate coefficient of halogenated aldehydes:

The halogenated aldehyde rate coefficients and lifetime data for the oxidants OH radicals and Cl atoms are presented in Tables S16 and S17, respectively. The halogenated aldehyde rate coefficient of $F(CF_2)_nCHO$ $(n = 1, 2, 3, 4, and\ 6)$ was determined by abstracting the hydrogen atom from the -CH(O) position, whereas for $CF_3(CH_2)_nCHO$ $(n = 1\ and\ 2)$, -H abstraction was feasible from both the $-CH_2$ and -CH(O) positions. Previous studies have indicated that the -CH(O) position is more favorable than the $-CH_2$ position in the case of $CF_3(CH_2)_nCHO$ $(n = 1\ and\ 2)$ halogenated aldehydes.[7] The reactivity of oxidants with halogenated aldehydes, such as $CClF_2CHO$, CCl_2FCHO, $CHClFCHO$, CCl_3CHO, $CHCl_2CHO$, and CH_2ClCHO, was examined by Sidebottom et al.[139] Their findings indicated that the rate coefficient for the reaction was reduced when halogen atoms were substituted for methyl hydrogens in acetaldehyde. The most electron-deficient locations are aldehydic hydrogens, which prefer radical attacks over halogen abstraction, as our ESP maps (Figure S11) also reveal. To validate the ESP diagram, we computed the bond dissociation energy (BDE) of $C_6F_{13}CH_2CHO$ at the B3LYP/6-311+G(d,p) level of theory. We found that the BDEs for aldehydic C-H bonds were approximately 93 kcal/mol, whereas those for -F bonds were approximately 107 kcal/mol. Overall, these findings explain the reported decreases in reactivity with successive halogen substitution and highlight the crucial role of aldehydic-H abstraction in determining the atmospheric degradation of halogenated aldehydes.

The fluoroaldehydes $F(CF_2)_nCHO$ $(n = 1, 2, 3, 4, and\ 6)$ react with OH radicals at rates that are over 30 times lower than acetaldehyde, according to published kinetic data, indicating substantial substituent effects.[140] Rayez et al.[141] identified two causes for these reactivity-suppressive factors: (i) a slight strengthening of the aldehydic C-H bond and (ii) instability of the transition state caused by the potent electron-withdrawing inductive action of the fluoroalkyl group. Similarly, in the case of $CF_3(CH_2)_nCHO$ $(n = 1\ and\ 2)$, the rate coefficient with OH radicals decreased by five times in comparison to $CH_3(CH_2)_nCHO$ $(n = 1\ and\ 2)$.[142] The decrease in the reactivity of the $\beta -$ and $\gamma -$ substituted fluorinated aldehyde must be due to the long-range destabilizing inductive action of the $-CF_3$ group in the transition state, as the aldehydic C-H bond strengths in these two molecules should be relatively comparable.[143] These tendencies are further supported by our FMO calculations, which show that fluorination in $F(CF_2)_nCHO$ $(n = 2, 3, 4, and\ 6)$ progressively increases the HOMO-LUMO energy gap, which is associated with decreased chemical reactivity. Together, our

View Article Online
DOI: 10.1039/D5EA00138B

results highlight that stronger C–H bonds are not the primary cause of the reduced atmospheric degradation of fluorinated aldehydes; electronic factors that destabilize the transition state and decrease radical accessibility also play a role. The table and figures are provided in the Supplementary Section, Table S15, and Figure S12.

3.3.2 Atmospheric fate of halogenated aldehydes:

Under atmospheric conditions, the fate of the byproducts of the photolysis and oxidation of halogenated aldehydes driven by OH radicals are of interest. The reaction with OH radicals produces CX_3CO radicals (X= H, F, Cl), whereas photolysis is predicted to form the CX_3 radical. In the troposphere, fully halogenated formaldehyde is photolytically stable, and its reaction with OH radicals is unimportant.[139] The degradation mechanisms of halogenated aldehydes, such as $F(CF_2)_nCHO$ $(n = 1, 2, 3, 4, and\ 6)$ and $CF_3(CH_2)_nCHO$ $(n = 1\ and\ 2)$ compounds, have been demonstrated in previous studies. For $F(CF_2)_nCHO$ $(n = 1, 2, 3, 4, and\ 6)$, alkyl radicals such as $F(CF_2)_nC(.)O$ $(n = 1, 2, 3, 4, \& 6)$ are produced via a picture (3.3.2.a.) illustrates the mechanism of deterioration of $F(CF_2)_nCHO$ $(n = 1, 2, 3, 4, and\ 6)$ via a single -H abstraction route involving an OH radical and a Cl atom. The following schematic is Scheme in 3.3.2.a. Degradation process of $F(CF_2)_nCHO$ $(n = 1, 2, 3, 4, and\ 6)$.

Furthermore, previously studied found that the degradation of $CF_3(CH_2)_nCHO$ $(n = 1\ and\ 2)$ compounds was investigated using aqueous-phase atmospheric degradation and UV photolysis in the actinic region (>290 nm).[7, 144] Similar to oxidizing radicals like the Cl atom and OH radical, $CF_3(CH_2)_nCHO$ $(n = 1\ \&\ 2)$ may be removed from the environment by UV photolysis.[7, 144] In addition, Sidebottom et al.[139] investigated the degradation of a variety of halogenated aldehydes ($CClF_2CHO$, CCl_2FCHO, $CHClFCHO$, CCl_3CHO, $CHCl_2CHO$, and CH_2ClCHO) in the environment

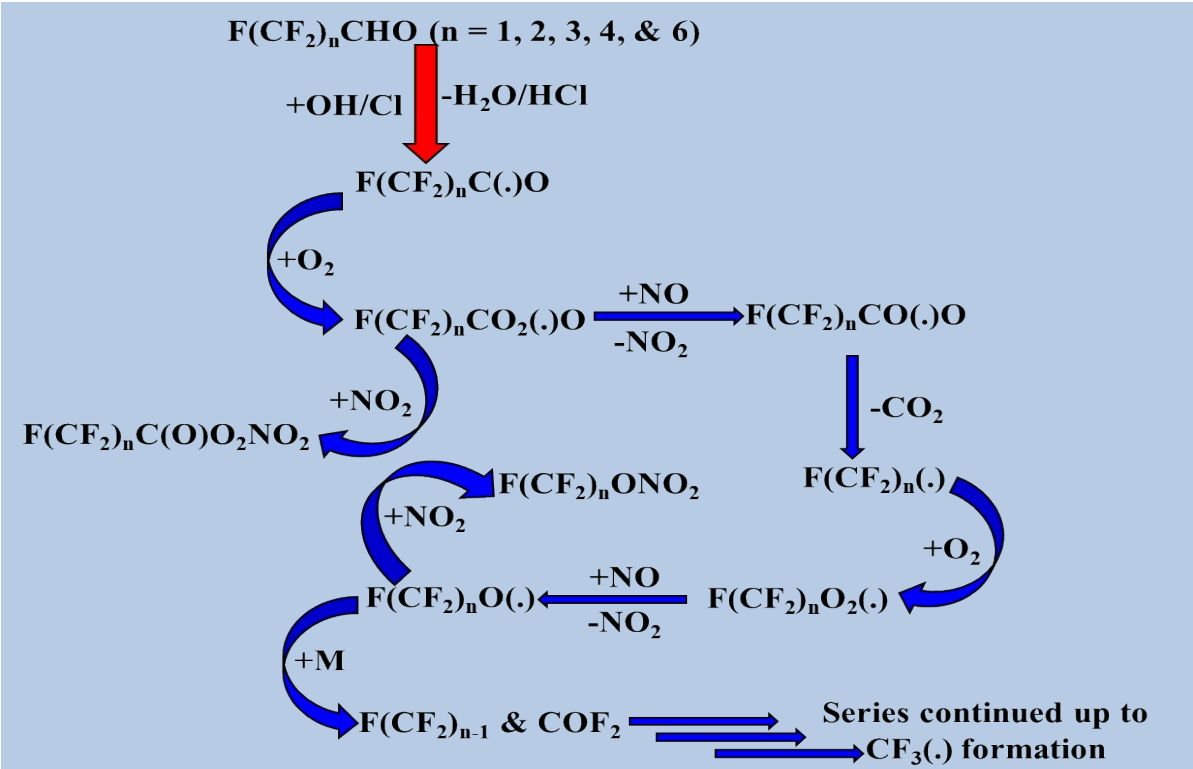

Scheme 3.3.2. a. Degradation process of $F(CF_2)_nCHO$ $(n = 1, 2, 3, 4, and\ 6)$.

View Article Online
DOI: 10.1039/D5EA00138B

and the reaction mechanism with OH radicals and Cl atoms. Initially, halogenated aldehydic hydrogen abstraction from oxidizing radicals was followed by the formation of the corresponding alkyl radicals. Two different mechanisms were observed: the first was decomposition, which was preferred if $X = Cl$, and the second was O_2 addition through the alkyl radical, as depicted in the schematic diagram (3.3.2. b.).

3.3.3 Atmospheric Implications of halogenated aldehydes:

The lifetimes of halogenated aldehydes with C-H bonds are primarily governed by oxidation reactions involving OH radicals and Cl atoms. The lifetimes of the 15 halogenated aldehydes are listed in Table S18. The total estimated atmospheric lifetime of different halogenated aldehydes was found to be the lowest at 0.00026 years for $CF_2CH_2CH_2CHO$, as calculated by Albaladejo et al.[7] and the highest at 0.36 years for CF_3CHO, as calculated by Nielsen *et al.*[140] In Table S16, we present the POCP values for halogenated aldehydes calculated by us. Almost all the studied halogenated aldehydes have negligible POCP values. Although the $CF_3CH_2CH_2CHO$ molecule exhibited a moderate POCP value of 31.7, its atmospheric emissions and ambient concentration were extremely low. Consequently, its overall contribution to tropospheric ozone formation is expected to be negligible, despite the moderate POCP value. To evaluate their radiative characteristics, GWP, and GTP, IR absorption cross-sections were calculated using vibrational frequencies and intensities, and geometries were optimized (see Figure S10 and Table S18). We found that $C_6F_{13}CH_2CHO$ had the most fluorine atoms, and its absorption intensity in the atmospheric window (700-1400 cm^{-1}) was higher than that of the other compounds, at approximately 2175 km/mol, wherease that of CH_2ClCHO was relatively low, at approximately 39 km/mol. We calculated the instantaneous and lifetime-corrected REs and GWPs of halogenated aldehydes over 20, 100, and 500 years, and the results are listed in Table S18. For most of the halogenated aldehydes, both the instantaneous and lifetime-corrected GWP values remains low. This is primarily because the presence of the aldehydic (H-C(O)-) hydrogen leads to a relatively fast reaction rate coefficient with atmospheric oxidants, resulting in a short atmospheric lifetime and consequently lower GWP values. The GTP (instantaneous and lifetime-corrected) values of 15 halogenated aldehydes over 20, 50, and 100-year time horizons were calculated for the first time and are reported in Table S19. Because of their low atmospheric lifetimes, most halogenated aldehyde compounds have negligible GTP values at 20, 50, and 100 years. However, six compounds ($CCl F_2CHO$, CCl_2FCHO, $CHClFCHO$, CCl_3CHO, $CHCl_2CHO$, and CH_2ClCHO), were examined to show detectable ozone-depletion potentials (ODPs) (see Table S19). Rainwater acidification may be caused by the

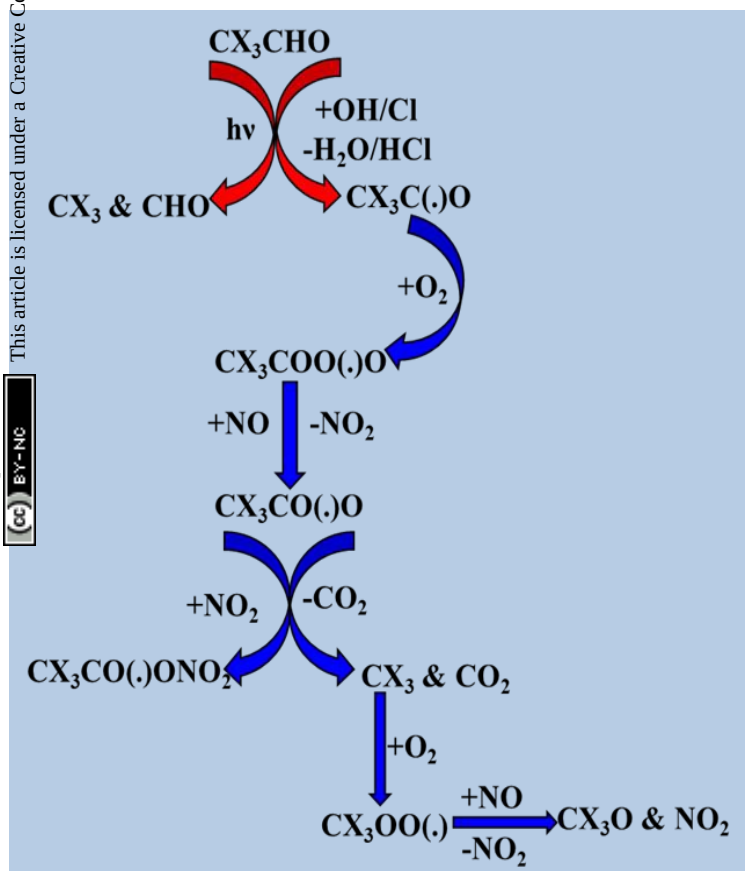

Scheme 3.3.2. b. Degradation process of CX_3CHO

View Article Online
DOI: 10.1039/D5EA00138B

breakdown products of halogenated aldehydes, as their acidification potentials (APs) are higher than those of SO_2. These results show that while the majority of halogenated aldehydes have an insignificant effect on the climate and ozone because of their short lives, their contribution to atmospheric acidification is also negligible due to their very low ambient concentrations.

3.4 Halogenated carboxylic acids

3.4.1 Rate coefficient of halogenated acids:

The rate coefficients of halogenated acids were explored via hydrogen abstraction from the -C (O)OH position of halogenated acids using OH radicals. Experimental studies by Hurley et al.[145] and Chen et al.[146] reported rate coefficients for $F(CF_2)_nCOOH$ $(n = 1, 2, 3, 4)$ with OH radicals are given in Supplementary Table S23. According to earlier research,[146] the transition states entail a hydrogen atom centered between the striking electrophilic OH radical and $CF_3C(O)O(.)$ radical, and the process involves hydrogen atom abstraction. When the CH_3 group was replaced with fluorine, the electron density on the H atom decreased, destabilizing the transition state compared to that with $CH_3C(O)OH$. ESP calculations (Figure S15) show that hydrogen atoms have electron-deficient region (red isosurfaces), making them more susceptible to H-abstraction by OH radicals. In contrast, fluorine substituents are surrounded by electron-rich areas, making abstraction even more difficult. The frontier molecular orbital (FMO) energy gap was analyzed, and the results are reported in Table S22 and illustrated in Figure S13, respectively.

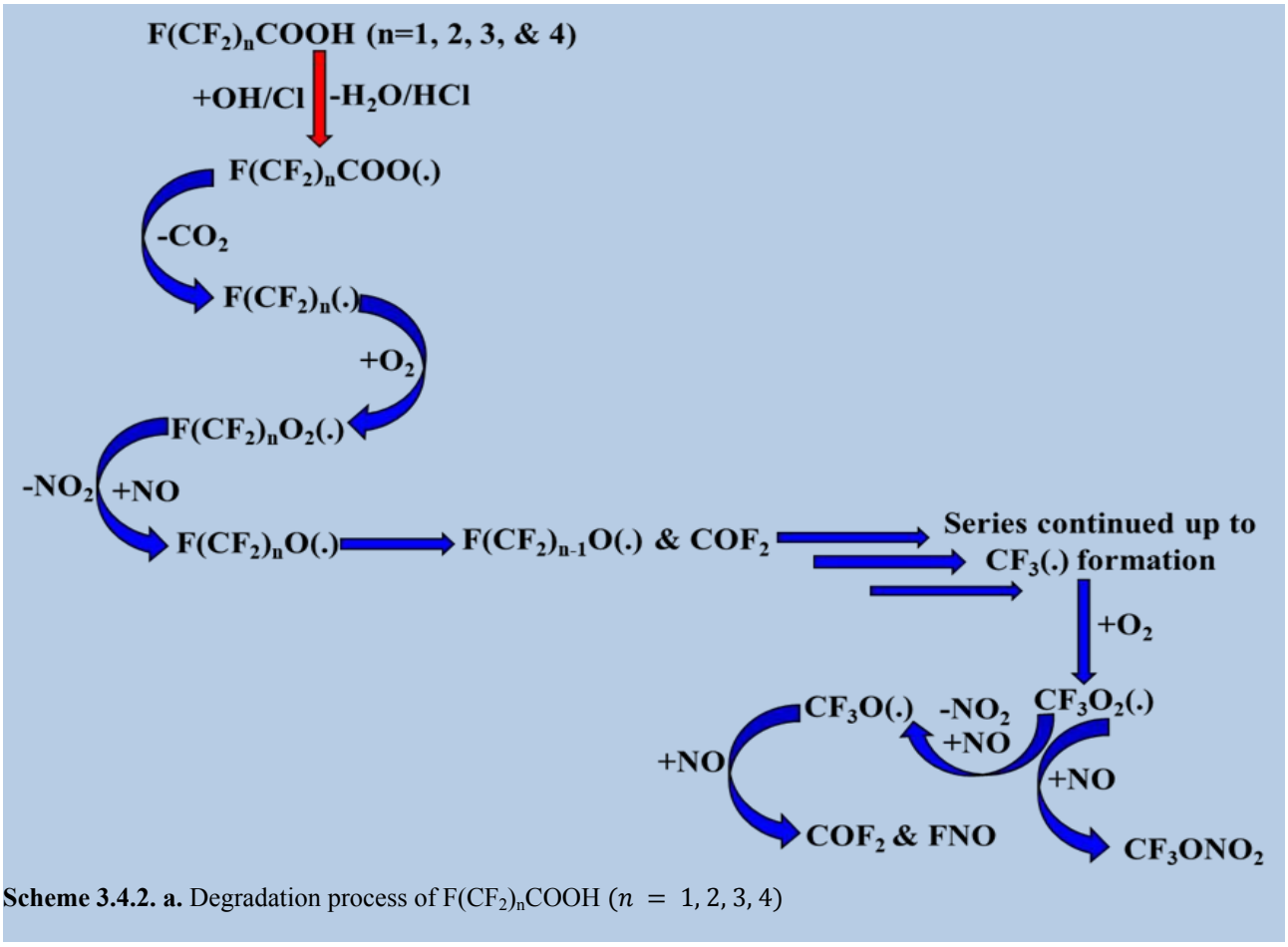

Scheme 3.4.2. a. Degradation process of $F(CF_2)_nCOOH$ $(n = 1, 2, 3, 4)$

3.4.2 Atmospheric fate of halogenated acids

Hurley *et al.*[145] and Chen *et al.*[146] previously examined how OH radicals break down halogenated

View Article Online
DOI: 10.1039/D5EA00138B

acids in the troposphere. We used their overall scheme from the preliminary findings, and it is evident from their scheme that radical products following hydrogen abstraction from halogenated acids were discovered in the schematic diagram (3.4.2.a). Owing to their thermodynamic stability, CO_2 molecules are released from halogenated acids following the formation of alkyl radicals, which form $F(CF_2)_n$ radicals. Finally, CF_3ONO_2, FNO, and COF_2 molecules are formed, as shown in the schematic diagram (3.4.2. a.).

3.4.3 Atmospheric Implications of halogenated acids

The lifetimes of halogenated carboxylic acids with C-H bonds are determined mainly by OH-driven and Cl-driven oxidation reactions. The lifetimes of the five halogenated carboxylic acids are listed in Table S24. These data were obtained from Hurley et al.[145], who studied the $F(CF_2)_nCOOH$ lifetime ($n = 1, 2, 3, 4$) and found that the lifetime ranges between 130-230 days. Chen *et al*.[146] also calculated the lifetime for i-C_4F_9COOH and reported it as 0.84 years. The reaction of $F(CF_2)_nCOOH$ with OH radicals is a minor contribution in atmospheric reaction. Wet and dry deposition is considered to be the main atmospheric removal mechanism for $F(CF_2)_nCOOH$, occurring on a timescale of approximately ten days.[145] In Table S23, we also mentioned the POCP values for halogenated carboxylic acids, which are negligible; therefore they have the least probability of creating tropospheric ozone. Figure S17 shows the absorption cross-section spectra of the halogenated carboxylic acids. According to Table S25, the predicted IR intensity in the atmospheric window increased with the number of fluorine atoms in the halogenated acids, leading to a corresponding increase in RE. We report the instantaneous and lifetime-corrected REs and GWP values of five halogenated carboxylic acids over 20, 100, and 500 years for the first time (Table S26). The GTP (lifetime-corrected and instantaneous) values of the five halogenated carboxylic acids were calculated over 20, 50, and 100 years for the first time and are tabulated in Table S27. For both cases, the instantaneous and lifetime-corrected GWP and GTP values were significant and may have impacted the atmosphere. The estimated AP values for halogenated carboxylic acids were higher than those of the reference compound SO_2.

3.5 Halogenated ketones and diketones

3.5.1 Rate coefficients of halogenated ketones and diketones:

The rate coefficients of halogenated ketones and diketones were determined through the -H abstraction via oxidants. Earlier research has found that the rate constants of halogenated aliphatic ketones are lower than those of non-halogenated aliphatic ketones. [147, 148] Wayne *et al*.[149] computed the rate coefficient in supplemental Table S30 and discovered that the rate constant value for the reaction with oxidizing radicals decreased when -CH_3 was entirely substituted by -CX_3 (X = F, Cl). It is possible that destabilizing polar effects in the transition state or modifications in the total enthalpy are responsible for the observed reduction in the reactivity upon acetone halogenation. The bond dissociation energy of the remaining C-H bonds in a methyl group decreases when an F/Cl atom is added in place of an H atom. [150] We computed the BDEs of $CHCl_2COCH_3$ at the B3LYP/6-311+G(d,p) level of theory, and our results are consistent with experimental findings. The BDEs for the dissociation of substituted methyl group-H bonds were approximately 88.2 kcal/mol, and for methyl group-H bonds, the BDEs were 99.8 kcal/mol.

Additionally, we computed the ESP diagrams for the halogenated ketones and diketones examined in this study (Supplemental Figure S19). Additionally, ESP maps were created for the halogenated ketones and diketones studied (Figure S19). These maps clearly demonstrate that H-abstraction from

View Article Online
DOI: 10.1039/D5EA00138B

electron-deficient regions is preferable to abstraction from halogen sites, which are surrounded by electron-rich zones. Consequently, hydrogen-atom abstraction is projected to occur preferentially from the halogenated methyl group rather than the unsubstituted methyl group, corresponding to the patterns indicated by the reaction enthalpies. According to previous studies, $CF_3CF_2CF_2C(O)CH_3$ and $CF_3CF_2CF_2CF_2C(O)CH_3$ have almost identical rate coefficients, which is expected because the size of the C_nF_{2n+1} group typically has an insignificant impact on the reactivity of halogenated ketones towards oxidizing radicals.[151] Regarding the rate coefficient of halogenated diketones, previous studies have demonstrated that the enol form exhibits significantly greater reactivity owing to the addition of oxidizing radicals to the C=C double bond, which is a dominant pathway compared to the H atom abstraction in the diketone forms. We also calculated the FMO energy gap, which is given in the supplementary section Table S29. Here, we discuss that the enol form exhibits electron density around the C=C bonds, as shown in Figure 2.

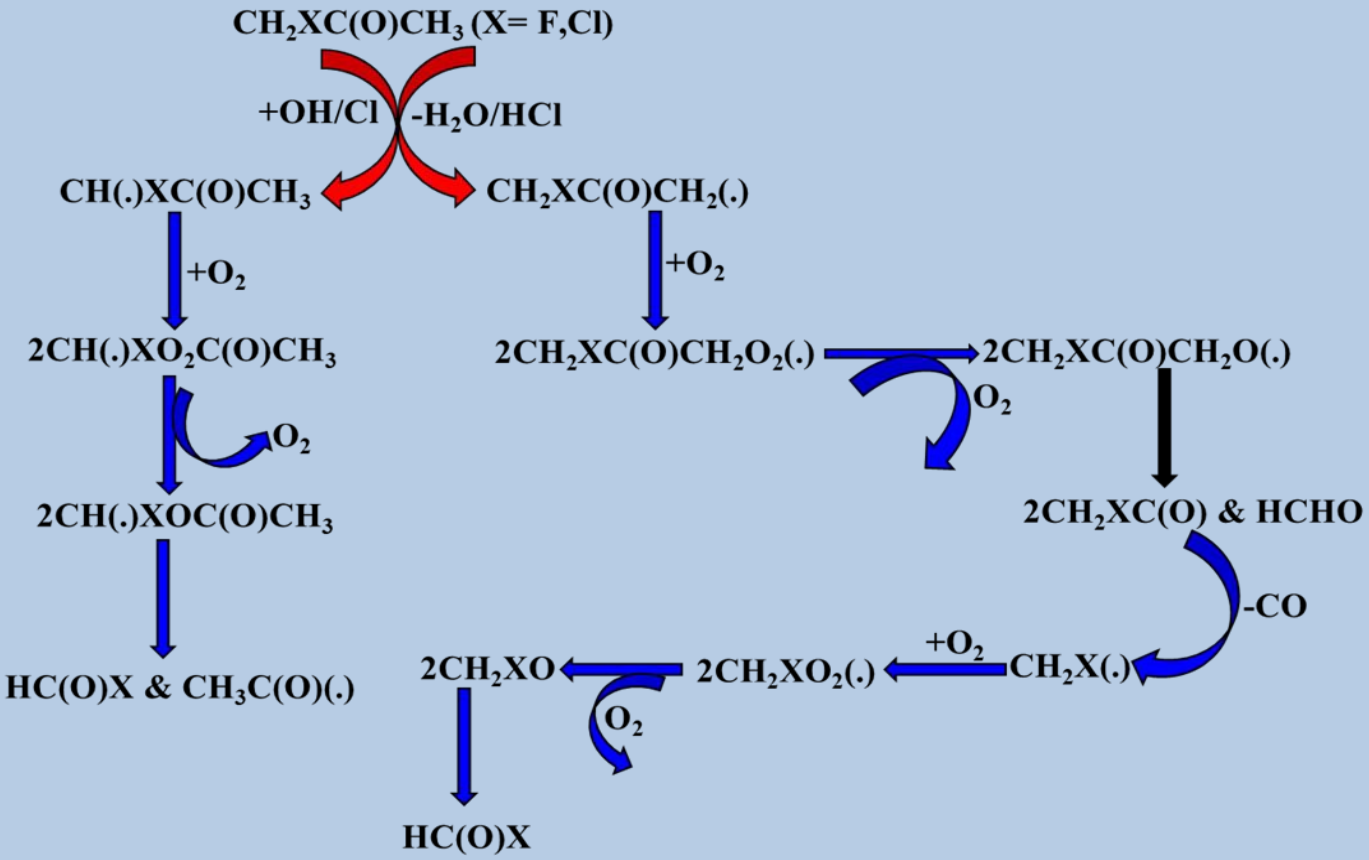

Scheme 3.5.2. a. Degradation process of $CH_2XC(O)CH_3$ (X= F, Cl)

View Article Online
DOI: 10.1039/D5EA00138B

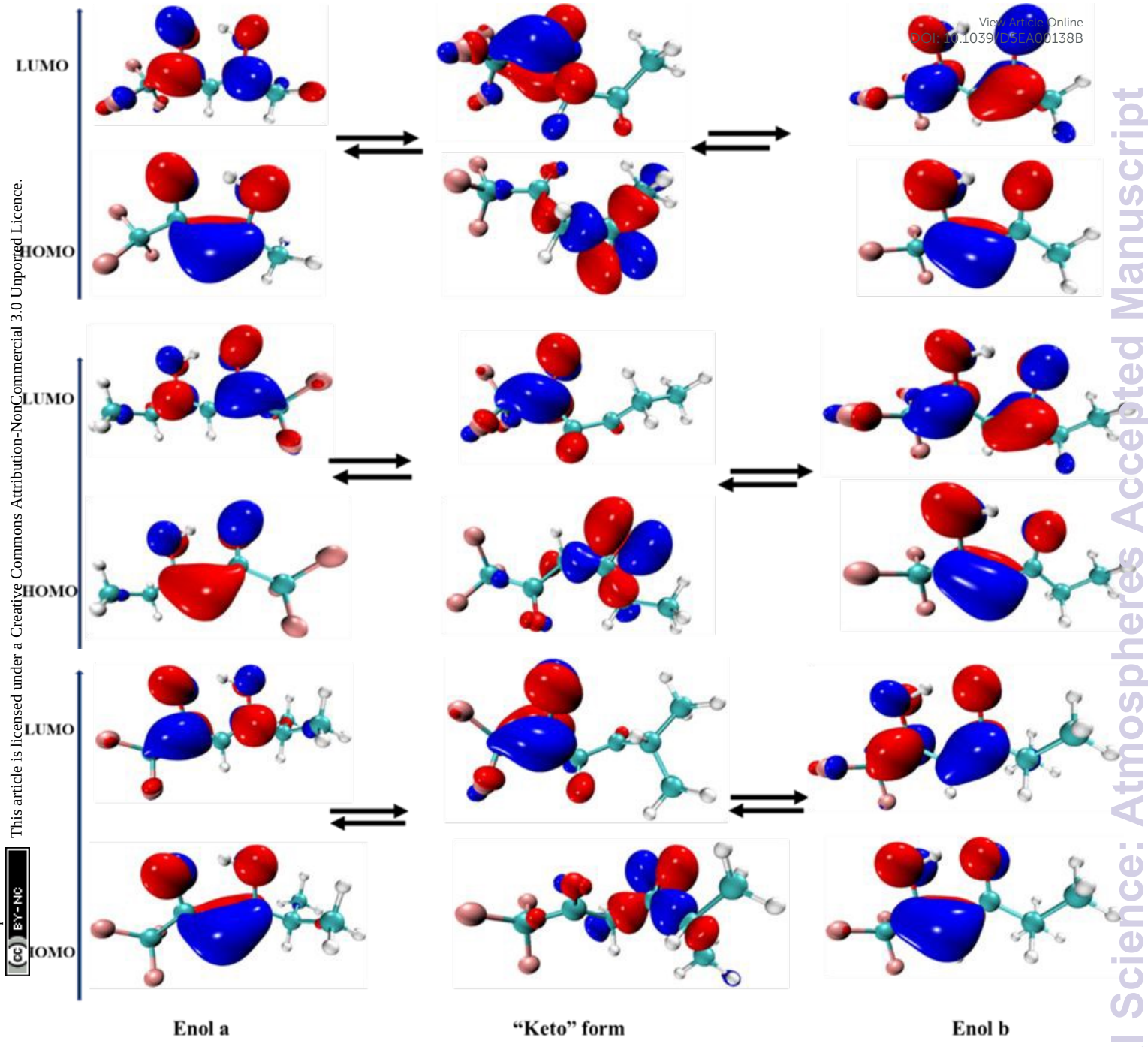

Figure 2. Analysis of Frontier molecular orbitals (FMO) in halogenated diketone (keto-enol tautomerization) compounds calculated at the B3LYP/6-311+G(d,p) level of theory.

3.5.2 Atmospheric fate of ketones and diketones

Following previous studies, [149] there are two ways in which OH radicals and Cl atoms attack partly halogenated substituted ketones: first, they extract hydrogen from the halogenated substituted methyl group, and second, they abstract hydrogen from the $-CH_3$ group. Both substituted and unsubstituted methyl groups in a monohalogenated ketone produced the same result, as shown in the schematic diagrams (3.5.2.a.). However, in the case of disubstituted halogenated ketones, the predicted outcome is HCOX when -H abstraction occurs through the methyl position, as shown in the schematic diagram of degradation pathways below,

View Article Online
DOI: 10.1039/D5EA00138B

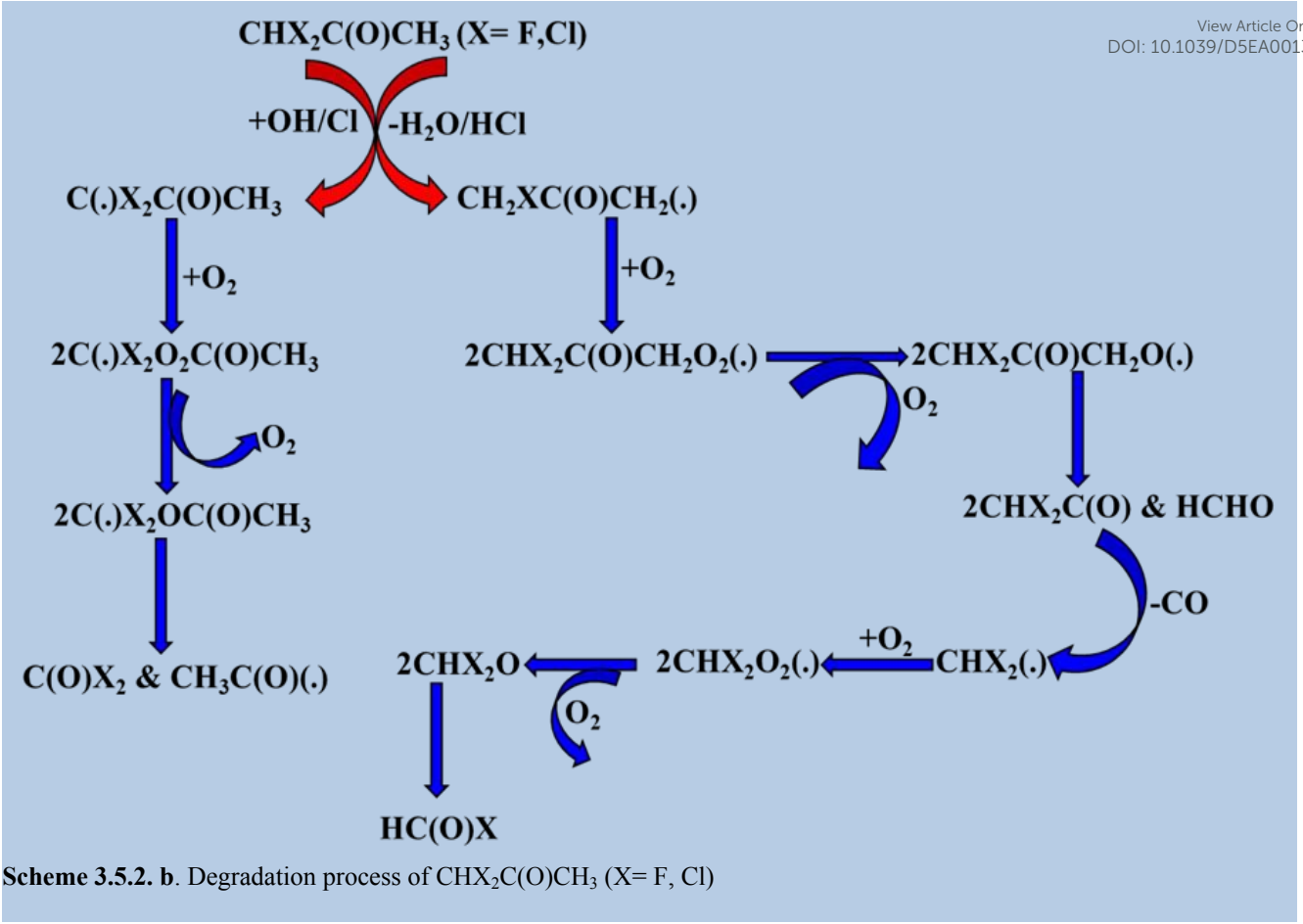

Scheme 3.5.2. b. Degradation process of $CHX_2C(O)CH_3$ (X= F, Cl)

and COX_2 when a reaction occurs with a substituted -CH_3 group.

The degradation of CX_3COCH_3 $(X = F, Cl)$ was also examined. Here, only one pathway is possible; that is, the hydrogen of the -CH_3 position is abstracted by the oxidizing radical to create the alkyl radical product $CX_3COCH_2(\cdot)$. According to the schematic chart, if X = Cl, CCl_3COCH_3 yields $COCl_2$ as its main byproduct, with a yield of nearly 100%. Moreover, a significant product was determined to be trifluoromethyl-glyoxal based on a comparison of the spectra, which revealed significant absorption bands at 1100–1300 cm^{-1} and 1813 cm^{-1}. The degradation processes of HC(O)F and $CH_3C(O)F$ involve OH radicals and Cl atoms, and both reactions with oxidizing radicals have low atmospheric relevance.[152, 153] The ability of halogenated diketones to change the position of double bonds inside their molecules by replacing an enol group with a single carbonyl moiety makes them noteworthy. The OH moiety and the carbonyl oxygen produce an intramolecular -H bond that stabilizes the enolic state. This type of isomerism is known as keto-enol tautomerism. [29] We conducted an NCI analysis to validate the experimental results. Green spikes are displayed in Figure 3, which are associated with hydrogen bonding between the OH moiety and carbonylic oxygen. As a result, the OH reaction with these compounds can occur either by attaching the OH radical to the double bond and H-abstraction in the enolic form or by H-abstraction in the keto form of the compound. Acetic acid, methyl glyoxal, and pentane-2,3,4-trione were found to be the identified main products of the OH radical-induced oxidation of enolic compounds in the gas phase.[29]

View Article Online
DOI: 10.1039/D5EA00138B

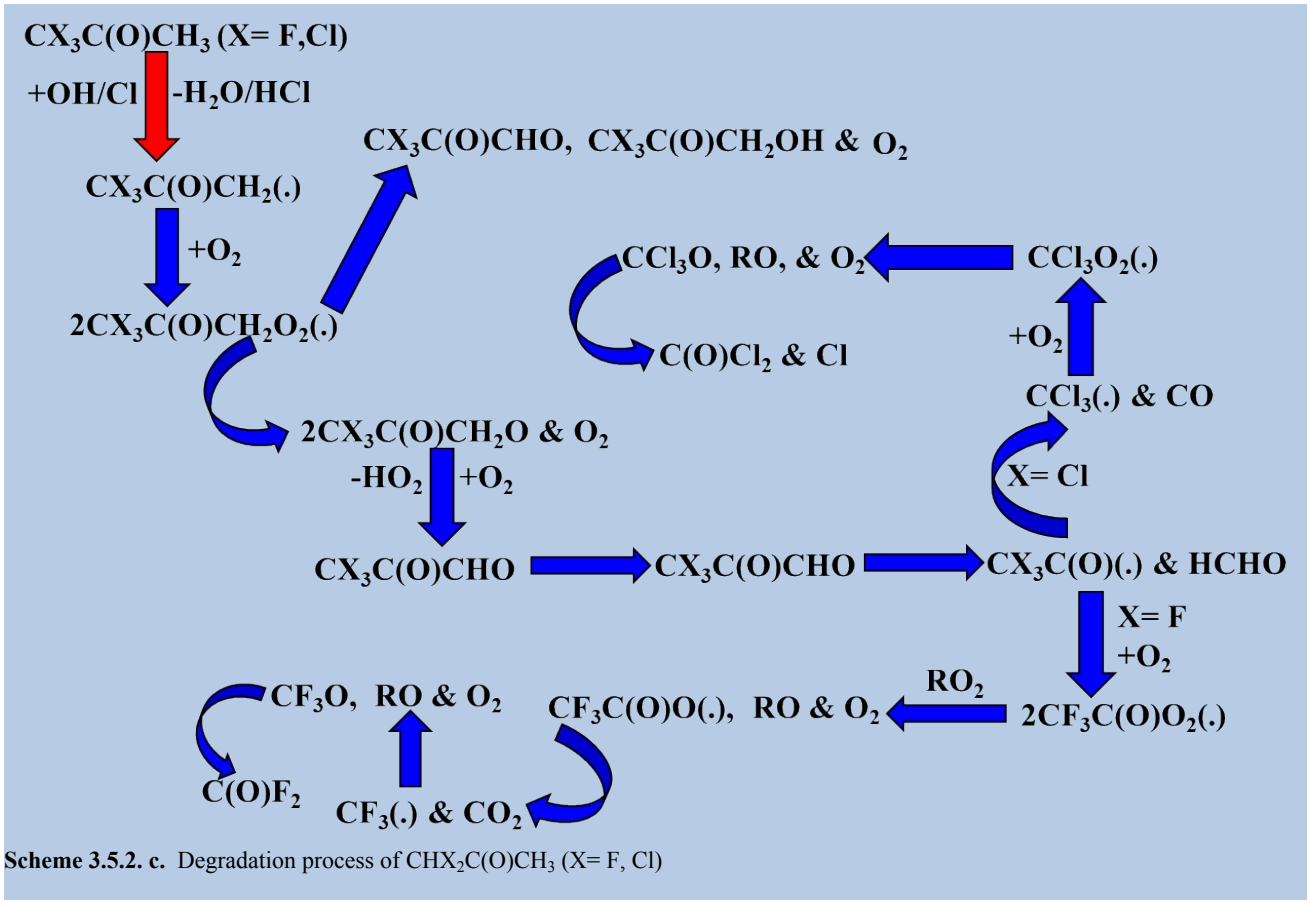

Scheme 3.5.2. c. Degradation process of $CHX_2C(O)CH_3$ (X= F, Cl)

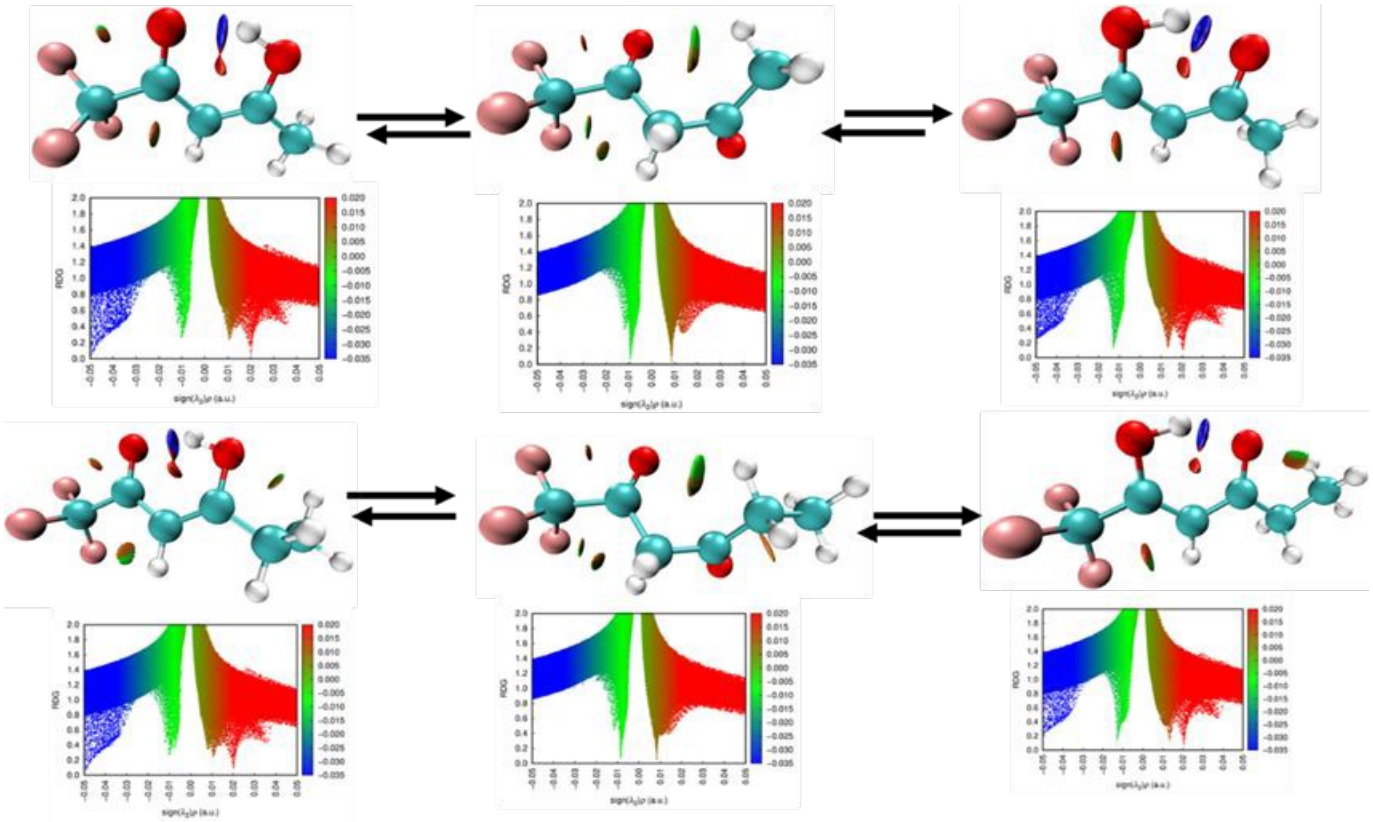

View Article Online
DOI: 10.1039/D5EA00138B

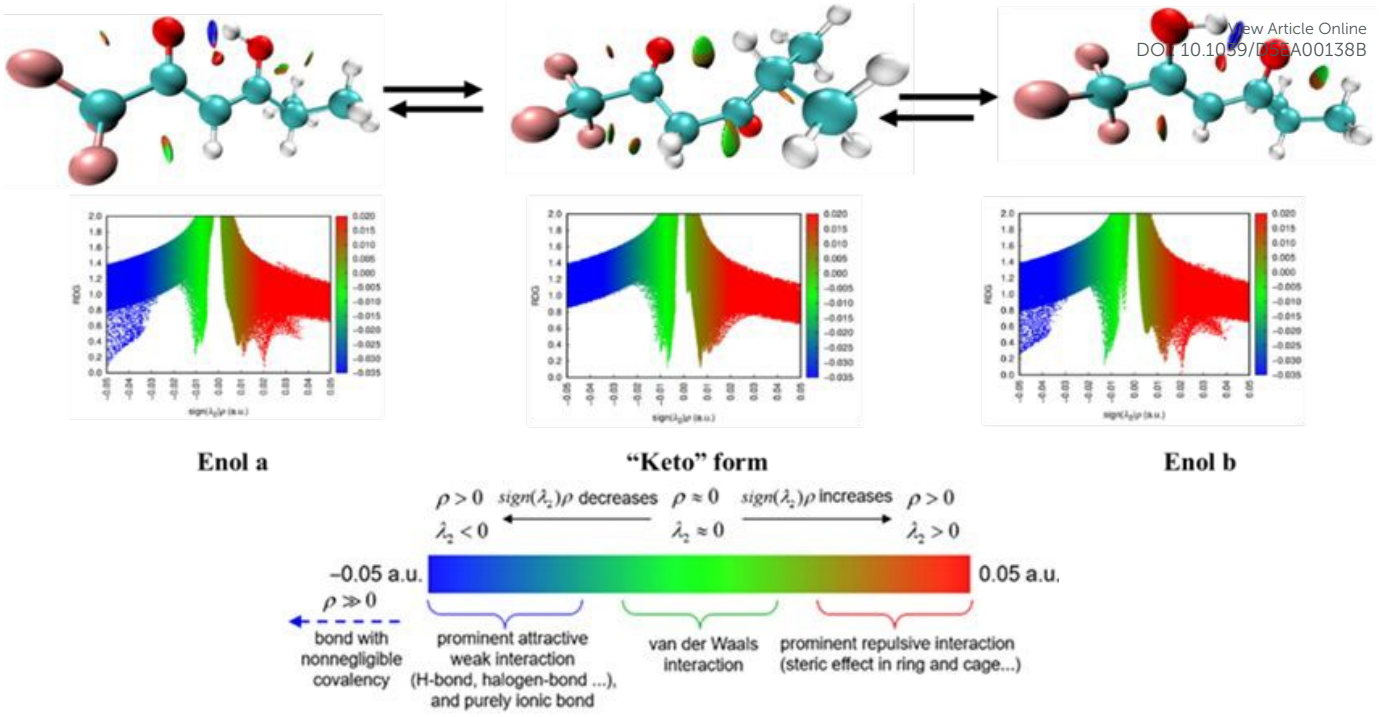

Figure 3. Analysis of non-covalent interactions (NCI) of halogenated diketone (keto-enol tautomerization) compounds calculated using the B3LYP method and 6-311+G(d,p) basis set.

3.5.3. Atmospheric Implications of halogenated ketones and diketones

The oxidation reaction by OH radicals and Cl atoms in the atmosphere is the primary removal process for halogenated ketones and diketones with C-H bonds. The lifetimes of the 13 halogenated ketones and diketones are listed in Table S31. Wayne *et al*.[149] calculated rate coefficient for $CF_3C(O)CH_3$, $CH_2FC(O)CH_3$, $CCl_3C(O)CH_3$, $CHCl_2C(O)CH_3$, $CH_2ClC(O)CH_3$, molecules. The lifetimes of these compounds were calculated using Equation S1. A and S1.B. The total estimated lifetimes of different halogenated ketones and diketones were found to be the lowest at 8 h for $CF_3C(O)CH_2C(O)CH(CH_3)_2$, as reported by Blanco *et al*.[29] and the highest at 9.31 y for $CF_3C(O)CH_3$, as reported by Wayne *et al*.[149] Our calculated POCP values of halogenated ketones and POCP values reported by Blanco *et al*.[29] for diketones are listed in Table S30. POCP values for ketones are negligible, but in the case of diketones ($CF_3C(O)CH_2C(O)CH_3$, $CF_3C(O)CH_2C(O)CH_2CH_3$, and $CF_3C(O)CH_2C(O)CH(CH_3)_2$), POCP values are significantly moderate based on reference compound ethene (100).

The optimization and frequency calculations in Table S32 indicate that successive fluorination systematically increases in RE. This pattern can be attributed to the fact that more fluorine atoms increase the absorption intensities in the atmospheric window (700-1400 cm^{-1}). The optimized molecular geometries of the halogenated ketones and diketones (Figure S18) reflect this tendency, and the projected IR spectra demonstrate that higher fluorine substitution leads to increased absorption characteristics in this important spectral region. The estimated absorption cross-section profiles (Figure S21) confirmed this improvement. We measured the immediate and lifetime-corrected REs and GWPs of 13 halogenated ketones and diketones across 20, 100, and 500-year time horizons (Table S33). Table S28 shows the immediate and lifetime-corrected

View Article Online
DOI: 10.1039/D5EA00138B

global temperature potentials (GTPs) of the same chemicals over 20, 50, and 100-year timeframes. Overall, our data show a strong relationship between increased fluorine substitution, greater IR absorption in the atmospheric window, and higher climate-relevant indices. We also calculated the ODP values of three chlorinated ketones ($CCl_3C(O)CH_3$, $CHCl_2C(O)CH_3$, and $CH_2ClC(O)CH_3$), and these values are summarized in Table S34. Table S34 shows that the AP values calculated and reported by Blanco *et al*.[29] were similar to those of SO_2. This indicates that halogenated ketones and diketones, as well as the products of their atmospheric degradation, may be involved in acid rain and are known to degrade water and soil quality, impacting the biota and human health.[154-156]

3.6. Summary of Atmospheric Metrics Across XOVOC Classes:

The findings in Table 1 show prominent structure-function correlations between the XOVOC classes. Halogenated alcohols have the highest atmospheric persistence (2d-46 y), often exceeding the lifetimes of typical hydrofluorocarbons, and thus contribute disproportionately to long-term climate forcing (GWP up to 3788). Halogenated aldehydes exhibit relatively short atmospheric lifetimes (4 days to approximately 0.36 years). Their reported POCP values (2.5-31.7), reference to ethene = 100, clearly indicate a low photochemical ozone creation potential. Moreover, their atmospheric concentrations are generally very low. Therefore, these compounds are not expected to contribute meaningfully to local or regional ozone formation, even under favorable photochemical condition. Halogenated esters have moderate lifetimes and GWPs, indicating a balance between structural stability and reactivity, whereas halogenated ketones and diketones have the greatest variability (8 h-10 y), highlighting their dual potential as both short-lived ozone precursors and longer-lived climate forcers. Halogenated acids, despite having a modest lifetime (130 days to 0.84 years), exhibit a comparatively higher acidification potential; however, their low atmospheric concentration implies that they are not expected to contribute significantly to large-scale atmospheric acidification. Overall, halogenated alcohols appear to be the most relevant to short-term effects on local air quality, whereas some carbonyl-containing species may also exert longer-term climatic impacts depending on their persistence and radiative properties.

Table 1. Typical ranges of atmospheric lifetimes (τ), GWP, POCP, and AP values for the representative classes of XOVOCs. And these OVOC classes are ordered based on lifetime ranges and their atmospheric matrices.

OVOCs Class	Lifetime (τ)	GWP (100 Year)	POCP	AP
Halogenated Alcohols	2 Days - 46 years	Less than 1 to 3788	0.4-17	0.50-1.22
Halogenated Ketone & Diketones	8 Hours - 10 years	Less than 1 to 1291	0.7-33.4	0.35-1.10
Halogenated Esters	5 Hours - 3.2 years	Less than 1 to 849	0.4 -32	0.35-1.09
Halogenated Acids	130 Days - 0.84 years	23-73	0.4-1.4	0.84-1.09
Halogenated Aldehydes	4 Days - 0.36 years	Less than 1 to 33	2.5-31.7	0.57-1.16

View Article Online
DOI: 10.1039/D5EA00138B

4. Dielectric Strength (DS):

One of the main issues with climate change is finding an environmentally friendly insulating gas to replace sulfur hexafluoride (SF_6), which has been an ongoing study in the past few years. The concern now is, why should alternatives replace SF_6? This is because the electric grid sector uses SF_6 extensively because of its exceptional insulating capabilities and chemical durability. [157] However, its GWP value is high, approximately 22500 times that of CO_2. Therefore, some suitable replacements that have confirmed exceptional qualities, such as high insulation strengths and low GWPs, are c-C_4F_8, CF_3I, $C_5F_{10}O$, $C_6F_{12}O$ (NOVEC 1230), and C_4F_7N.[157] A new sustainable insulating gas called NOVEC 1230 has been developed recently.[158] In this review, our chosen high-thought-out computational approaches include the B3LYP/6-311+G(d,p) level of theory, which is superior to PBE1PBE, M06-2X, and M11 methods that were previously established through a broad range of organic compounds for DS prediction.[106] Furthermore, it is remarkable that halogenated OVOCs of interest require adding polarization and diffuse functions to the minimal basis sets for the following reasons. (i) Polarization function: These compounds have multiple chemical bonds and soft nature. (ii) Diffuse function: For neutral and cationic systems, DFT calculations predict one of the important variables, namely the ionization energy. (iii) To balance the computational accuracy and efficiency, the diffuse functions of substantial elements must be used preferentially. Considering

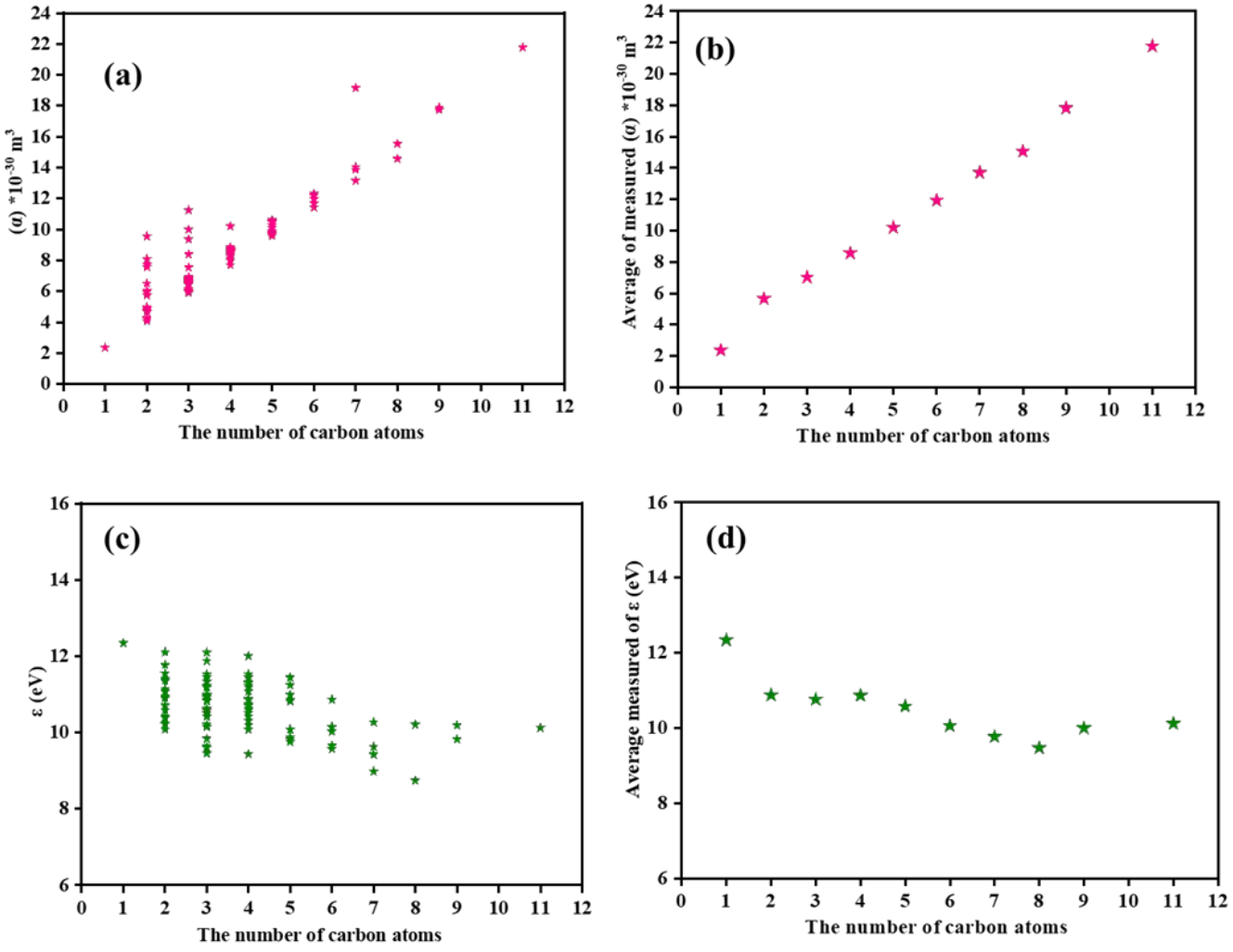

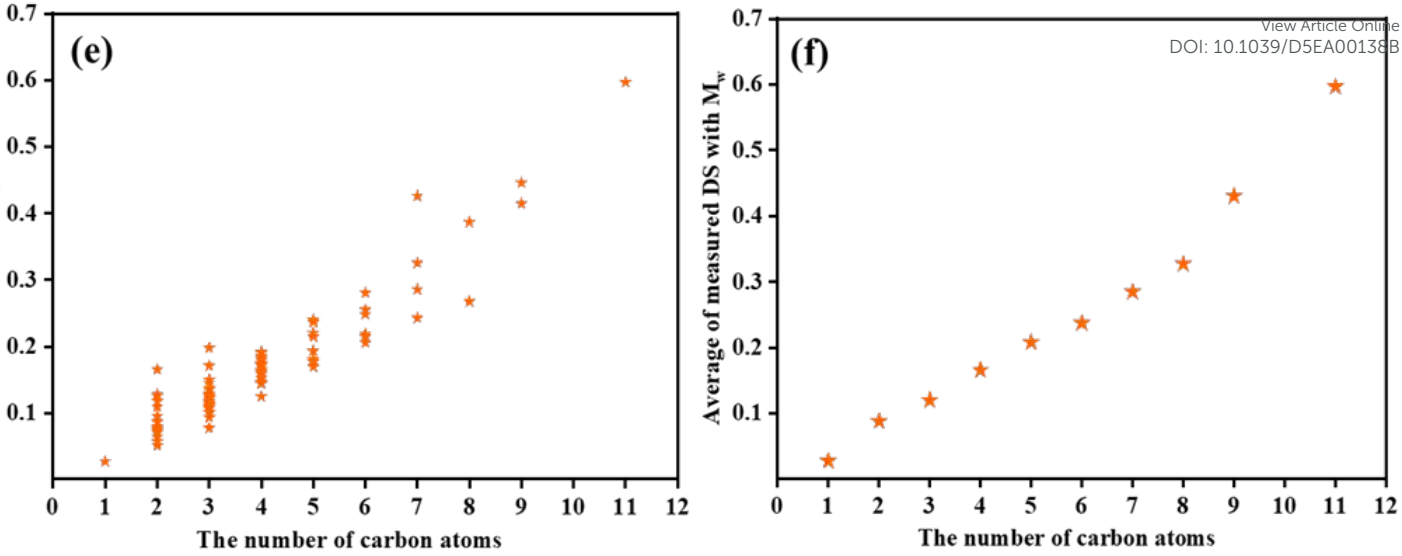

Figure 4. Correlations with physical characteristics of the participants. (a, b) Polarizabilities, (c, d) ionization energies, and (e, f) and dielectric strengths of halogenated OVOCs correlated with the number of carbon atoms.

all factors, the 6-311+G(d,p) basis set was the most

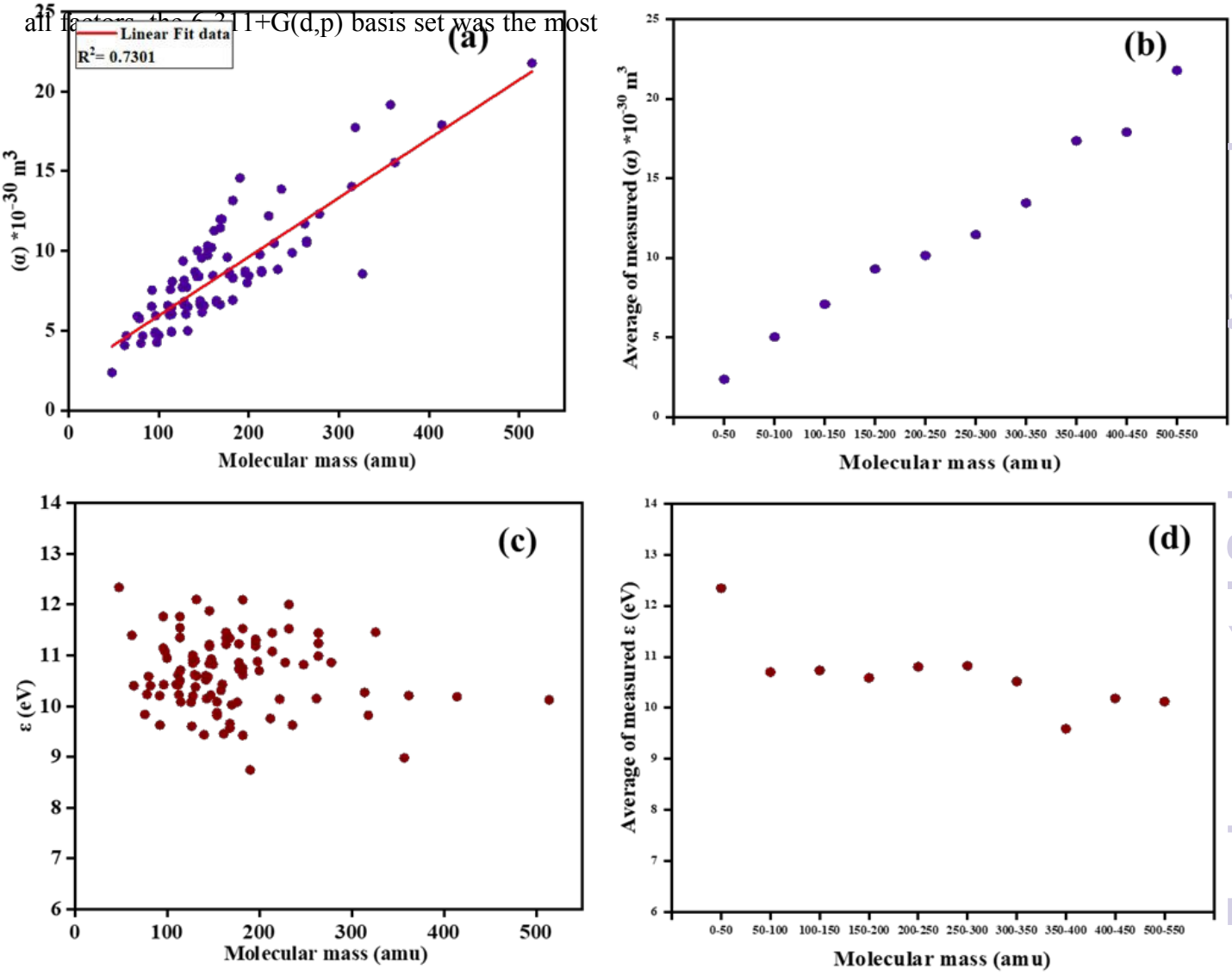

View Article Online
DOI: 10.1039/D5EA00138B

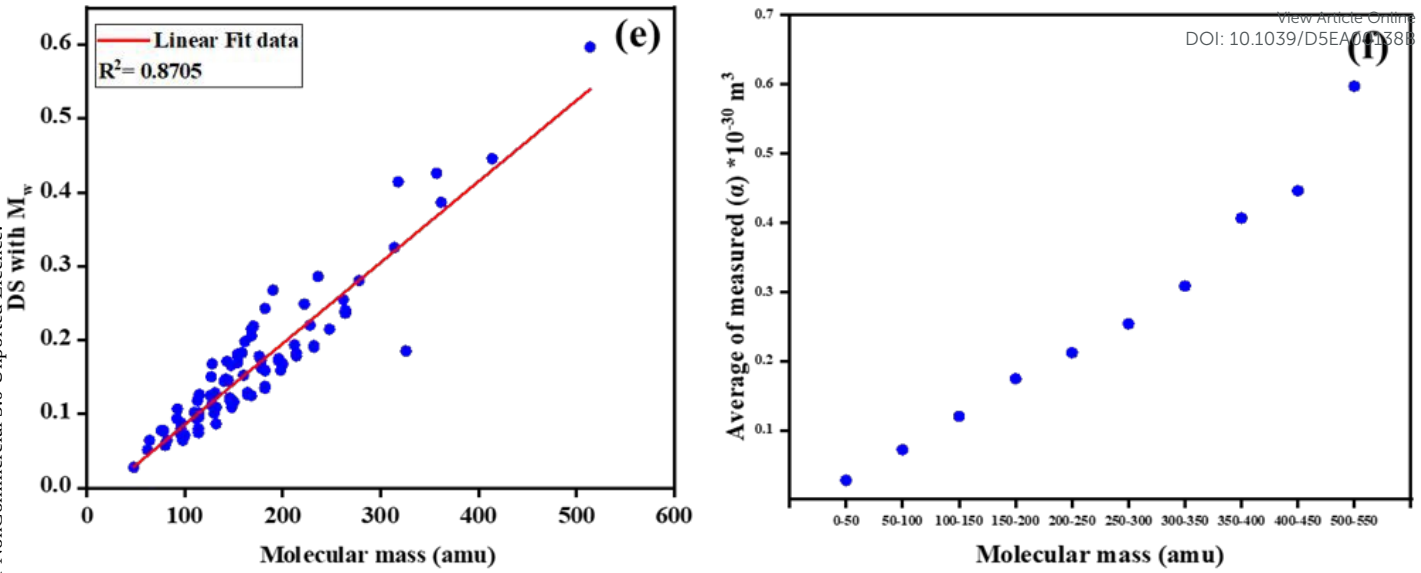

Figure 5. Correlations with physical characteristics of the participants. (a, b) Polarizabilities, (c, d) ionization energies, and (e, f) dielectric strengths of the halogenated OVOCs correlated with their molecular weight.

appropriate for this investigation.[106] As shown in the figures, there is a wide range of halogenated esters, alcohols, aldehydes, acids, ketones, and diketones. The polarizability increases linearly with molecular weight and backbone length (number of carbon atoms), as shown in Figures 5 and 6, whereas the ionization energy is insensitive to these structural characteristics. Furthermore, the dielectric strength shows a linear relationship with molecular weight and backbone length, owing to the unique characteristics of the two fundamental variables (polarizability and ionization energy) that define DS. Supplementary Tables S7, S14, S21, S28, and S35 list the theoretically determined DS, polarizability, and ionization energy values for XOVOCs.

4.1. Survey of SF_6 Alternatives:

The demand for insulation gases in industrial applications are extremely high, includes aspects such as dielectric performance, chemical and thermal stability, non-flammability, cost-effectiveness, durability, and an ecologically friendly design.[159] An ideal insulation gas would be a substance that minimally impacts the atmospheric environment, endures electric fields corresponding to the highest voltage levels, and satisfies safety, risk, and toxicity requirements for equipment operating under all conceivable circumstances.[160] In this context, our assessment of XOVOCs offers atmospheric lifetimes, RE, GWP, and POCP metrics that are specifically relevant to preliminary environmental examinations such as minimal impact on the atmosphere. Efforts to replace SF_6 in electrical equipment have yielded compounds that can be utilized as pure gas. However, no single gas has been identified as the most suitable option for all requirements. Extensive screening studies, such as those assessing halogenated alcohols, ketones, and associated compounds, have investigated a wide array of candidates for SF_6 substitution. None of them fulfills the complete set of dielectrics, chemical, thermal, safety, and environmental requirements needed for dependable use in high-voltage equipment, even if some have qualities that make them appropriate for use as pure gases.

5. Conclusion

We reviewed the reactions of halogenated oxygenated volatile organic compounds (XOVOCs) with Cl atoms and OH radical oxidants. However, based on our prior findings, we have concluded that

View Article Online
DOI: 10.1039/D5EA00138B

hydroxyl radicals often control daytime chemistry in the troposphere and, to a certain extent, in natural water. The OH radical's high oxidative capability makes it a "detergent of the atmosphere." Compared to other oxidative species, hydroxyl radicals are highly reactive, causing most tropospheric trace chemicals and contaminants to undergo oxidation and chemical conversion. This review presents an extensive database on the kinetics and mechanistic degradation pathways of the gas-phase oxidation of XOVOCs. Based on these data, we concluded that some significant general predictions regarding the reaction rate coefficients and degradation pathway mechanisms for OVOCs could be established. From this reviewed data, we have found their atmospheric implications; we provide an extensive evaluation of the lifetimes of 94 oxygenated hydrofluorocarbons, including fluorinated and chlorinated (esters, alcohols, aldehydes, and ketones), fluorinated carboxylic acids, and fluorinated diketones, which absorb IR radiation and disturb the Earth's radiation budget. For halogenated esters, the lifetime value decreased with the addition of hydrogen atoms to the molecules. Halogenated esters had the highest lifetime values among the 94 oxygenated hydrofluorocarbons considered in this study. The instantaneous and lifetime-corrected REs of 105 compounds were summarized, among which we calculated the REs of 46 compounds for the first time, which have not been studied yet. We also summarized the GWP values in both cases, instantaneous and lifetime-corrected values of 94 oxygenated hydrofluorocarbons over 20, 100, and 500 years' time horizons, among which the GWP values of 46 compounds were reported for the first time. The GWP values of some oxygenated hydrofluorocarbons are significantly high over a 20-year time horizon, which is a concern. This review article also contains a thorough compilation of instantaneous and lifetime-corrected GTP values of 94 oxygenated hydrofluorocarbon compounds over 20-, 50-, and 100-year time horizons, among which the GTPs of 59 compounds were calculated. The GTP values of some halogenated ketones are considerably high. The ODPs of 14 chlorine-containing oxygenated hydrofluorocarbons were also calculated by us and reported for the first time. The calculated ODP values for chlorine-containing oxygenated hydrofluorocarbons were considerably low. In this review, we calculated the POCP and AP values for almost all the OVOCs considered. The POCP values were negligible for the considered halogenated compounds, and some had moderate POCP values such as $CF_3CH_2CH_2CHO$, diketones, and unsaturated halogenated esters. Despite their moderate POCP values, the atmospheric impact of these XOVOCs was negligible. Their low emission rates from industrial sources prevent any significant contribution to tropospheric ozone or smog formation; thus, they may not fall under stringent air quality regulations. Overall, the structural class of XOVOCs determines their atmospheric effects; alcohols and ketones with longer lives exert greater climatic forcing (GWP), whereas esters and aldehydes are more significant for short-term air quality (POCP, AP) than alcohols and ketones. Although the high acidification potential (AP) of XOVOCs is a noted characteristic, implying a theoretical risk of contributing to water acidification after degradation, their environmental impact is negligible. This is because of their very low atmospheric concentration. This article reviews XOVOC chemicals, their rate coefficients, mechanistic pathways, and their atmospheric implications. Although we determined their dielectric strength (DS), which is crucial for identifying substitutes for SF_6 molecules with high GWP values that negatively impact the atmosphere, no one can substitute this SF_6 molecule based on our calculations.

Author Information

Kanika Guleria: Conceptualization, Methodology, Writing-original draft preparation, Formal analysis, Reviewing, and Editing.

Suresh Tiwari: Conceptualization, Methodology, Writing-original draft preparation, Formal analysis, Reviewing, and Editing.

Ranga Subramanian: Conceptualization, Methodology, Formal Analysis, Supervision, Reviewing, and Editing.

Acknowledgment

S.T. thanks the Indian Institute of Technology Patna for providing research facilities and financial support to carry out this work.

References:

1. Ø. Hodnebrog, M. Etminan, J. Fuglestvedt, G. Marston, G. Myhre, C. Nielsen, K. P. Shine and T. Wallington, *Reviews of Geophysics*, 2013, **51**, 300-378.
2. J. E. Hansen and M. Sato, *Proceedings of the National Academy of Sciences*, 2001, **98**, 14778-14783.
3. V. Papadimitriou, *Journal of Science Education and Technology*, 2004, **13**, 299-307.
4. S. Solomon and J. S. Daniel, *Climatic Change*, 1996, **32**, 7-17.
5. G. Ghani, *Economics Bulletin*, 2007, **17**, 1-5.
6. M. Grubb, C. Vrolijk and D. Brack, *Routledge revivals: Kyoto Protocol (1999): A guide and assessment*, Routledge, 2018.
7. M. Antiñolo, E. Jiménez, A. Notario, E. Martínez and J. Albaladejo, *Atmospheric Chemistry and Physics*, 2010, **10**, 1911-1922.
8. N. K. Gour, K. Borthakur, S. Paul and R. C. Deka, *Chemosphere*, 2020, **238**, 124556.
9. G. J. Velders, S. Solomon and J. S. Daniel, *Atmospheric Chemistry and Physics*, 2014, **14**, 4563-4572.
10. D. Gielen and T. Kram, 1998.
11. Y. Ninomiya, M. Kawasaki, A. Guschin, L. Molina, M. Molina and T. Wallington, *Environmental science & technology*, 2000, **34**, 2973-2978.
12. L. Chen, S. Kutsuna, K. Tokuhashi and A. Sekiya, *The Journal of Physical Chemistry A*, 2006, **110**, 12845-12851.
13. M. Sulbaek Andersen, O. Nielsen, T. Wallington, M. Hurley and W. DeMore, *The Journal of Physical Chemistry A*, 2005, **109**, 3926-3934.
14. D. Zehavi and J. N. Seiber, *Analytical Chemistry*, 1996, **68**, 3450-3459.
15. H. Frank, A. Klein and D. Renschen, *Nature*, 1996, **382**, 34-34.
16. A. Jordan and H. Frank, *Environmental science & technology*, 1999, **33**, 522-527.
17. C. E. Wujcik, D. Zehavi and J. N. Seiber, *Chemosphere*, 1998, **36**, 1233-1245.
18. B. Baidya, M. Lily and A. K. Chandra, *ChemistrySelect*, 2019, **4**, 7134-7143.
19. A. Garzón, M. Moral, A. Notario, A. A. Ceacero-Vega, M. Fernández-Gómez and J. Albaladejo, *ChemPhysChem*, 2010, **11**, 442-451.
20. T. Kelly, V. Bossoutrot, I. Magneron, K. Wirtz, J. Treacy, A. Mellouki, H. Sidebottom and G. Le Bras, *The Journal of Physical Chemistry A*, 2005, **109**, 347-355.
21. M. Hurley, T. Wallington, M. Sulbaek Andersen, D. Ellis, J. Martin and S. Mabury, *The Journal of Physical Chemistry A*, 2004, **108**, 1973-1979.
22. M. D. Hurley, J. A. Misner, J. C. Ball, T. J. Wallington, D. A. Ellis, J. W. Martin, S. A. Mabury and M. Sulbaek Andersen, *The Journal of Physical Chemistry A*, 2005, **109**, 9816-9826.
23. S. R. Sellevåg, C. J. Nielsen, O. A. Søvde, G. Myhre, J. K. Sundet, F. Stordal and I. S. Isaksen, *Atmospheric Environment*, 2004, **38**, 6725-6735.
24. T. J. Wallington, M. P. Sulbaek Andersen and O. J. Nielsen, in *Advances in atmospheric chemistry*, World Scientific, 2017, pp. 305-402.
25. M. De Rosa, D. Arnold, D. Hartline, L. Truong, R. Verner, T. Wang and C. Westin, *The Journal of Organic Chemistry*, 2015, **80**, 12288-12299.
26. R. Ilmi, A. Haque, I. J. Al-Busaidi, N. K. Al Rasbi and M. S. Khan, *Dyes and Pigments*, 2019, **162**, 59-66.

DOI: 10.1039/D5EA00138B

27. V. G. Isakova, S. K. Tat'yana and F. A. Lakhvich, *Russian Chemical Reviews*, 2010, **79**, 849.
28. V. Babain, V. Romanovskii, V. Starchenko, A. Shadrin, G. Kudinov, S. Podoinitsyn and Y. Revenko, *Journal of Nuclear Science and Technology*, 2002, **39**, 267-269.
29. P. L. Lugo, V. Straccia, C. B. Rivela, I. Patroescu-Klotz, N. Illmann, M. A. Teruel, P. Wiesen and M. B. Blanco, *Chemosphere*, 2022, **286**, 131562.
30. D. A. Ellis, S. A. Mabury, J. W. Martin and D. C. Muir, *Nature*, 2001, **412**, 321-324.
31. M. Lily, S. Hynniewta, B. Muthiah, W. Wang, A. K. Chandra and F. Liu, *Atmospheric Environment*, 2021, **249**, 118247.
32. D. Good, J. Francisco, A. Jain and D. J. Wuebbles, *Journal of Geophysical Research: Atmospheres*, 1998, **103**, 28181-28186.
33. Ø. Hodnebrog, B. Aamaas, J. S. Fuglestvedt, G. Marston, G. Myhre, C. J. Nielsen, M. Sandstad, K. P. Shine and T. J. Wallington, *Reviews of Geophysics*, 2020, **58**, e2019RG000691.
34. I. Bravo, Y. Díaz-de-Mera, A. Aranda, E. Moreno, D. R. Nutt and G. Marston, *Physical Chemistry Chemical Physics*, 2011, **13**, 17185-17193.
35. P. Zhu, X.-m. Duan and J.-y. Liu, *Journal of Fluorine Chemistry*, 2015, **176**, 61-70.
36. G. Srinivasulu, S. Vijayakumar and B. Rajakumar, *ChemistrySelect*, 2018, **3**, 4480-4489.
37. G. Solignac, A. Mellouki, G. Le Bras, M. Yujing and H. Sidebottom, *Physical Chemistry Chemical Physics*, 2007, **9**, 4200-4210.
38. L. P. Viegas, *Atmosphere*, 2022, **13**, 1256.
39. J. B. Burkholder, R. Cox and A. Ravishankara, *Chemical Reviews*, 2015, **115**, 3704-3759.
40. K. Tokuhashi, K. Takizawa and S. Kondo, *Environmental Science and Pollution Research*, 2018, **25**, 15204-15215.
41. V. Schmidt, G.-Y. Zhu, K. Becker and E. Fink, 1984.
42. T. Schaefer, J. Schindelka, D. Hoffmann and H. Herrmann, *The Journal of Physical Chemistry A*, 2012, **116**, 6317-6326.
43. H. Herrmann, *Chemical reviews*, 2003, **103**, 4691-4716.
44. B. Ervens, S. Gligorovski and H. Herrmann, *Physical Chemistry Chemical Physics*, 2003, **5**, 1811-1824.
45. D. Hoffmann, B. Weigert, P. Barzaghi and H. Herrmann, *Physical Chemistry Chemical Physics*, 2009, **11**, 9351-9363.
46. H. Herrmann, D. Hoffmann, T. Schaefer, P. Bräuer and A. Tilgner, *ChemPhysChem*, 2010, **11**, 3796-3822.
47. K. Tokuhashi, A. Takahashi, M. Kaise, S. Kondo, A. Sekiya and E. Fujimoto, *Chemical Physics Letters*, 2000, **325**, 189-195.
48. K. Tokuhashi, L. Chen, K. Takizawa, A. Takahashi, T. Uchimaru, M. Sugie, S. Kondo and A. Sekiya, *Fluorine Chemistry Research Advances*, 2007, 143-241.
49. R. Simonaitis and J. Heicklen, *International Journal of Chemical Kinetics*, 1973, **5**, 231-241.
50. G. J. Doyle, A. C. Lloyd, K. Darnall, A. M. Winer and J. N. Pitts Jr, *Environmental Science & Technology*, 1975, **9**, 237-241.
51. J. G. Calvert, A. Lazrus, G. L. Kok, B. G. Heikes, J. G. Walega, J. Lind and C. A. Cantrell, *Nature*, 1985, **317**, 27-35.
52. H. Niki, P. Maker, C. Savage and L. Breitenbach, *The Journal of Physical Chemistry*, 1978, **82**, 132-134.
53. K. R. Darnall, R. Atkinson and J. N. Pitts Jr, *The Journal of Physical Chemistry*, 1978, **82**, 1581-1584.
54. C. J. Young, M. D. Hurley, T. J. Wallington and S. A. Mabury, *Journal of Geophysical Research: Atmospheres*, 2008, **113**.
55. P. J. Godin, A. Cabaj, S. Conway, A. C. Hong, K. Le Bris, S. A. Mabury and K. Strong, *Journal of Molecular Spectroscopy*, 2016, **323**, 53-58.
56. G. Myhre, C. Nielsen, D. Powell and F. Stordal, *Atmospheric Environment*, 1999, **33**, 4447-4458.
57. P. J. Godin, A. Cabaj, L.-H. Xu, K. Le Bris and K. Strong, *Journal of Quantitative*

Spectroscopy and Radiative Transfer, 2017, **186**, 150-157.
58. F.-Y. Liu, Z.-W. Long, X.-F. Tan and B. Long, *Computational and Theoretical Chemistry*, 2014, **1038**, 33-39.
59. L. Yang, J. Y. Liu, L. Wang, H. Q. He, Y. Wang and Z. S. Li, *Journal of Computational Chemistry*, 2008, **29**, 550-561.
60. L. Yang, J. Y. Liu, S. Q. Wan and Z. S. Li, *Journal of Computational Chemistry*, 2009, **30**, 565-580.
61. F.-Y. Bai, G. Sun, X. Wang, Y.-Q. Sun, R.-S. Wang and X.-M. Pan, *The Journal of Physical Chemistry A*, 2015, **119**, 1256-1266.
62. T.-X. Chi, X.-X. Li, S. Ni, F.-Y. Bai, X.-M. Pan and Z. Zhao, *Physical Chemistry Chemical Physics*, 2024, **26**, 24821-24832.
63. S. Tiwari and R. Subramanian, *Physical Chemistry Chemical Physics*, 2025.
64. M. Frisch, G. Trucks, H. B. Schlegel, G. Scuseria, M. Robb, J. Cheeseman, G. Scalmani, V. Barone, G. Petersson and H. Nakatsuji, *Journal*, 2016.
65. R. Dennington, T. Keith and J. Millam, 2009.
66. Y. Zhao and D. G. Truhlar, *Theoretical chemistry accounts*, 2008, **120**, 215-241.
67. Y. Zhao and D. G. Truhlar, *Accounts of chemical research*, 2008, **41**, 157-167.
68. Y. Zhao and D. G. Truhlar, *The Journal of chemical physics*, 2006, **125**.
69. A. D. Becke, *Journal of chemical Physics*, 1993, **98**, 1372-1377.
70. K. Guleria and R. Subramanian, *ACS Earth and Space Chemistry*, 2023, **7**, 947-959.
71. K. Guleria and R. Subramanian, *Theoretical Chemistry Accounts*, 2022, **141**, 77.
72. K. Guleria and R. Subramanian, *Computational and Theoretical Chemistry*, 2022, **1208**, 113547.
73. S. Begum and R. Subramanian, *RSC Advances*, 2015, **5**, 39110-39121.
74. Y. Zhao and D. G. Truhlar, *Theoretical chemistry accounts*, 2008, **120**, 215-241.
75. J. Pal and R. Subramanian, *Physical Chemistry Chemical Physics*, 2019, **21**, 6525-6534.
76. C. Gonzalez and H. B. Schlegel, *The Journal of Chemical Physics*, 1989, **90**, 2154-2161.
77. C. Gonzalez and H. B. Schlegel, *Journal of Physical Chemistry*, 1990, **94**, 5523-5527.
78. J. A. Pople, M. Head-Gordon and K. Raghavachari, *The Journal of chemical physics*, 1987, **87**, 5968-5975.
79. B. C. Garrett and D. G. Truhlar, *The Journal of Chemical Physics*, 1979, **70**, 1593-1598.
80. B. C. Garrett and D. G. Truhlar, *Journal of the American chemical Society*, 1979, **101**, 4534-4548.
81. B. C. Garrett, D. G. Truhlar, R. S. Grev and A. W. Magnuson, *The Journal of Physical Chemistry*, 1980, **84**, 1730-1748.
82. D. G. Truhlar and A. Kuppermann, *Journal of the American Chemical Society*, 1971, **93**, 1840-1851.
83. A. Fernandez-Ramos, B. A. Ellingson, B. C. Garrett and D. G. Truhlar, *Reviews in computational chemistry*, 2007, **23**, 125.
84. D.-h. Lu, T. N. Truong, V. S. Melissas, G. C. Lynch, Y.-P. Liu, B. C. Garrett, R. Steckler, A. D. Isaacson, S. N. Rai and G. C. Hancock, *Computer Physics Communications*, 1992, **71**, 235-262.
85. Y. P. Liu, G. C. Lynch, T. N. Truong, D. H. Lu, D. G. Truhlar and B. C. Garrett, *Journal of the American Chemical Society*, 1993, **115**, 2408-2415.
86. A. Virmani, M. P. Walavalkar, A. Sharma, S. Sengupta, A. Saha and A. Kumar, *Atmospheric environment*, 2020, **237**, 117709.
87. K. Guleria and R. Subramanian, *ACS Earth and Space Chemistry*, 2022, **6**, 1596-1611.
88. I. Bravo, G. Marston, D. R. Nutt and K. P. Shine, *Journal of Quantitative Spectroscopy and Radiative Transfer*, 2011, **112**, 1967-1977.
89. I. Bravo, A. Aranda, M. D. Hurley, G. Marston, D. R. Nutt, K. P. Shine, K. Smith and T. J. Wallington, *Journal of Geophysical Research: Atmospheres*, 2010, **115**.
90. P. Blowers and K. Hollingshead, *The Journal of Physical Chemistry A*, 2009, **113**, 5942-5950.

View Article Online
DOI: 10.1039/D5EA00138B

DOI: 10.1039/D5EA00168B

91. V. C. Papadimitriou and J. B. Burkholder, *The Journal of Physical Chemistry A*, 2016, **120**, 6618-6628.
92. P. J. Godin, K. Le Bris and K. Strong, *Journal of Quantitative Spectroscopy and Radiative Transfer*, 2017, **203**, 522-529.
93. K. Strong, P. J. Godin, K. Le Bris, H. Johnson, R. Piunno, A. Cabaj, C. MacDougall and L.-H. Xu, 2018.
94. P. Blowers, K. F. Tetrault and Y. Trujillo-Morehead, *Theoretical Chemistry Accounts*, 2008, **119**, 369-381.
95. Z. Li, Z. Tao, V. Naik, D. A. Good, J. C. Hansen, G. R. Jeong, J. S. Francisco, A. K. Jain and D. J. Wuebbles, *Journal of Geophysical Research: Atmospheres*, 2000, **105**, 4019-4029.
96. K. Le Bris, J. DeZeeuw, P. J. Godin and K. Strong, *Journal of Quantitative Spectroscopy and Radiative Transfer*, 2017, **203**, 538-541.
97. P. J. Godin, H. Johnson, R. Piunno, K. Le Bris and K. Strong, *Journal of Quantitative Spectroscopy and Radiative Transfer*, 2019, **225**, 337-350.
98. S. Tiwari and R. Subramanian, *Theoretical Chemistry Accounts*, 2024, **143**, 1-15.
99. K. Guleria, S. Tiwari, D. Barman, S. Daschakraborty and R. Subramanian, *Electron Density: Concepts, Computation and DFT Applications*, 2024, 527-549.
100. A. D. Becke, *Physical review A*, 1988, **38**, 3098.
101. T. Lu and F. Chen, *Journal of computational chemistry*, 2012, **33**, 580-592.
102. H. William, *Journal of molecular graphics*, 1996, **14**, 33-38.
103. J. Tirado-Rives and W. L. Jorgensen, *Journal of chemical theory and computation*, 2008, **4**, 297-306.
104. K. E. Riley, B. T. Op't Holt and K. M. Merz, *Journal of chemical theory and computation*, 2007, **3**, 407-433.
105. C. Y. Go and K. C. Kim, *The Journal of Physical Chemistry A*, 2024.
106. J. Jang, K. H. Jung and K. C. Kim, *Scientific Reports*, 2022, **12**, 7027.
107. T. Wallington, W. Schneider, J. Sehested, M. Bilde, J. Platz, O. Nielsen, L. Christensen, M. Molina, L. Molina and P. Wooldridge, *The Journal of Physical Chemistry A*, 1997, **101**, 8264-8274.
108. L. Chen, S. Kutsuna, K. Tokuhashi and A. Sekiya, *Chemical physics letters*, 2004, **400**, 563-568.
109. L. Chen, S. Kutsuna, K. Tokuhashi and A. Sekiya, *International journal of chemical kinetics*, 2004, **36**, 337-344.
110. S. Urata, T. Uchimaru, A. K. Chandra, A. Takada and A. Sekiya, *International journal of chemical kinetics*, 2002, **34**, 524-530.
111. A. K. Chandra, T. Uchimaru, M. Sugie and A. Sekiya, *Chemistry letters*, 2002, **31**, 132-133.
112. N. Oyaro, S. R. Sellevåg and C. J. Nielsen, *Environmental science & technology*, 2004, **38**, 5567-5576.
113. L. Christensen, J. Sehested, O. Nielsen, M. Bilde, T. Wallington, A. Guschin, L. Molina and M. Molina, *The Journal of Physical Chemistry A*, 1998, **102**, 4839-4845.
114. C. M. Tovar and M. A. Teruel, *Atmospheric Environment*, 2014, **94**, 489-495.
115. M. B. Blanco and M. A. Teruel, *Atmospheric Environment*, 2007, **41**, 7330-7338.
116. M. B. Blanco, I. Bejan, I. Barnes, P. Wiesen and M. A. Teruel, *Chemical Physics Letters*, 2008, **453**, 18-23.
117. N. K. Gour, R. C. Deka, H. J. Singh and B. K. Mishra, *Journal of Fluorine Chemistry*, 2014, **160**, 64-71.
118. T. J. Wallington, P. Dagaut, R. Liu and M. J. Kurylo, *International Journal of Chemical Kinetics*, 1988, **20**, 177-186.
119. A. El Boudali, S. Le Calvé, G. Le Bras and A. Mellouki, *The Journal of Physical Chemistry*, 1996, **100**, 12364-12368.
120. S. Le Calve, G. Le Bras and A. Mellouki, *The Journal of Physical Chemistry A*, 1997, **101**, 5489-5493.
121. K. G. Kambanis, Y. G. Lazarou and P. Papagiannakopoulos, *The Journal of Physical Chemistry A*, 1998, **102**, 8620-8625.
122. I. W. Smith and A. Ravishankara, *The Journal of Physical Chemistry A*, 2002, **106**, 4798-4807.

123. M. B. Blanco, C. Rivela and M. A. Teruel, *Chemical Physics Letters*, 2013, **578**, 33-37.
124. T. Stein, L. Christensen, J. Platz, J. Sehested, O. Nielsen and T. Wallington, *The Journal of Physical Chemistry A*, 1999, **103**, 5705-5713.
125. M. Gnanaprakasam, L. Sandhiya and K. Senthilkumar, *The Journal of Physical Chemistry A*, 2018, **122**, 9316-9325.
126. V. G. Straccia C, A. L. Cardona, M. a. B. Blanco, O. N. Ventura and M. Teruel, *ACS Earth and Space Chemistry*, 2024.
127. A. Rodríguez, I. Bravo, D. Rodríguez, M. Tajuelo, Y. Diaz-de-Mera and A. Aranda, *RSC advances*, 2016, **6**, 21833-21843.
128. C. M. Butt, C. J. Young, S. A. Mabury, M. D. Hurley and T. J. Wallington, *The Journal of Physical Chemistry A*, 2009, **113**, 3155-3161.
129. A. Garzon, M. Antinolo, M. Moral, A. Notario, E. Jimenez, M. Fernandez-Gomez and J. Albaladejo, *Molecular Physics*, 2013, **111**, 753-763.
130. G. Srinivasulu and B. Rajakumar, *The Journal of Physical Chemistry A*, 2013, **117**, 4534-4544.
131. F.-Y. Bai, Y.-J. Liu, X. Wang, Y.-Q. Sun and X.-M. Pan, *RSC Advances*, 2016, **6**, 63954-63964.
132. F.-Y. Bai, X. Wang, Y.-Q. Sun, R.-S. Wang and X.-M. Pan, *RSC advances*, 2016, **6**, 36096-36108.
133. V. L. Orkin, V. G. Khamaganov and M. J. Kurylo, *The Journal of Physical Chemistry A*, 2012, **116**, 6188-6198.
134. M. Lily and A. K. Chandra, *Journal of Fluorine Chemistry*, 2015, **175**, 185-192.
135. A. Kumar, S. Gonu, S. Vijayakumar, C. Ramya and B. Rajakumar, *The Journal of Physical Chemistry A*, 2021, **125**, 523-535.
136. F.-Y. Bai, M.-S. Deng, M.-Y. Chen, L. Kong, S. Ni, Z. Zhao and X.-M. Pan, *Physical Chemistry Chemical Physics*, 2021, **23**, 13115-13127.
137. B. Baidya, M. Lily and A. K. Chandra, *ChemistrySelect*, 2018, **3**, 6136-6144.
138. X. Wang, D. J. Jacob, S. D. Eastham, M. P. Sulprizio, L. Zhu, Q. Chen, B. Alexander, T. Sherwen, M. J. Evans and B. H. Lee, *Atmospheric Chemistry and Physics*, 2019, **19**, 3981-4003.
139. D. Scollard, J. Treacy, H. Sidebottom, C. Balestra-Garcia, G. Laverdet, G. LeBras, H. MacLeod and S. Teton, *The Journal of Physical Chemistry*, 1993, **97**, 4683-4688.
140. S. R. Sellevåg, T. Kelly, H. Sidebottom and C. J. Nielsen, *Physical Chemistry Chemical Physics*, 2004, **6**, 1243-1252.
141. M. T. Rayez, J. C. Rayez, T. Berces and G. Lendvay, *The Journal of Physical Chemistry*, 1993, **97**, 5570-5576.
142. R. Atkinson, *J. Phys. Chem. Ref. Data, Monograph*, 1994, **2**, 1-216.
143. D. F. McMillen and D. M. Golden, *Annu. Rev. Phys. Chem.;(United States)*, 1982, **33**.
144. M. Antiñolo, E. Jimenez and J. Albaladejo, *Journal of Photochemistry and Photobiology A: Chemistry*, 2012, **231**, 33-40.
145. M. Hurley, M. Sulbaek Andersen, T. Wallington, D. Ellis, J. Martin and S. Mabury, *The Journal of Physical Chemistry A*, 2004, **108**, 615-620.
146. L. Chen, T. Uchimaru, S. Kutsuna, K. Tokuhashi and A. Sekiya, *Chemical Physics Letters*, 2011, **514**, 207-213.
147. G. Vasvári, I. Szilágyi, Á. Bencsura, S. Dóbe, T. Bérces, E. Henon, S. Canneaux and F. Bohr, *Physical Chemistry Chemical Physics*, 2001, **3**, 551-555.
148. S. Vandenberk, L. Vereecken and J. Peeters, *Physical Chemistry Chemical Physics*, 2002, **4**, 461-466.
149. S. Carr, D. E. Shallcross, C. E. Canosa-Mas, J. C. Wenger, H. W. Sidebottom, J. J. Treacy and R. P. Wayne, *Physical Chemistry Chemical Physics*, 2003, **5**, 3874-3883.
150. D. R. Lide, *CRC handbook of chemistry and physics*, CRC press, 2004.
151. J. Calvert, 2011.
152. X. Song, G. b. L. Zügner, M. Farkas, Á. Illés, D. Sarzynski, T. Rozgonyi, B. Wang and S. Dóbé, *The Journal of Physical Chemistry A*, 2015, **119**, 7753-7765.
153. T. J. Wallington and M. D. Hurley, *Environmental science & technology*, 1993, **27**, 1448-1452.

View Article Online
DOI: 10.1039/D5EA00138B

View Article Online
DOI: 10.1039/D5EA00138B

154. A. Bouwman, D. Van Vuuren, R. Derwent and M. Posch, *Water, Air, and Soil Pollution*, 2002, **141**, 349-382.
155. D. Granados Sánchez, G. López Ríos and M. Hernández García, *Revista Chapingo serie ciencias forestales y del ambiente*, 2010, **16**, 187-206.
156. H. Huang, *International journal of environmental studies*, 1992, **41**, 267-275.
157. Y. Yang, K. Gao, L. Ding, J. Bi, S. Yuan and X. Yan, *High Voltage*, 2021, **6**, 733-749.
158. J. Pagliaro and G. Linteris, *Fire Safety Journal*, 2017, **87**, 10-17.
159. M. Rabie and C. M. Franck, *Environmental science & technology*, 2018, **52**, 369-380.
160. X. Li, H. Zhao and A. B. Murphy, *Journal of Physics D: Applied Physics*, 2018, **51**, 153001.

All required data is provided in the supplementary information.

View Article Online
DOI: 10.1039/D5EA00138B